Characterization of Ethylene/α-Olefin Copolymers Made with a Single-Site Catalyst Using Crystallization Elution Fractionation

by

Abdulaal Alkhazaal

A thesis
presented to the University of Waterloo
in fulfillment of the
thesis requirement for the degree of
Master of Applied Science

in

Chemical Engineering

Waterloo, Ontario, Canada, 2011

AUTHOR'S DECLARATION

I hereby declare that I am the sole author of this thesis. This is a true copy of the thesis, including any required final revisions, as accepted by my examiners.

I understand that my thesis may be made electronically available to the public.

Abstract

A new analytical technique to measure the chemical composition distribution (CCD) of polyolefins, crystallization elution fractionation (CEF), was introduced in 2006 during the *First International Conference on Polyolefin Characterization*. CEF is a faster and higher resolution alternative to the previous polyolefin CCD analytical techniques such as temperature rising elution fractionation (TREF) and crystallization elution fractionation (CRYSTAF) (Monrabal et al., 2007).

Crystallization elution fractionation is a liquid chromatography technique used to determine the CCD of polyolefins by combining a new separation procedure, dynamic crystallization, and TREF. In a typical CEF experiment, a polymer solution is loaded in the CEF column at high temperature, the polymer is allowed to crystallize by lowering the solution temperature, and then the precipitated polymer is eluted by a solvent flowing through the column as the temperature is raised. CEF needs to be calibrated to provide quantitative CCD results.

A CEF calibration curve consists of a mathematical relationship between elution temperature determined by CEF and comonomer fraction in the copolymer that could be estimated by Fourier transform infrared spectroscopy (FTIR) and carbon-13 nuclear magnetic resonance (^{13}C NMR). Different comonomer types in ethylene/α-olefin copolymers will have distinct calibration curves.

The main objective of this thesis is to obtain CEF calibration curves for several different ethylene/α-olefin copolymers and to investigate which factors influence these calibration curves. A series of homogeneous ethylene/α-olefin copolymers (1-hexene, 1-octene and 1-dodecene) with different comonomer fractions were synthesized under controlled conditions to create CEF calibration standards. Their average chemical compositions were determined by ^{13}C NMR and FTIR and then used to establish CEF calibration curves relating elution temperature and comonomer molar fraction in the copolymer.

Acknowledgements

My most incompetent gratitude is to Allah, the Almighty who have directed me in every component of this work and my life in his unlimited gifts, wisdom and perception.

My continuous thanks go to my parents and my wife for their love, support and incentive. They did their best to encourage me to finish this project.

I am extremely grateful and thankful to my supervisor Prof. Joao Soares who gave me the opportunity to become one of his students. I thank him for giving me the chance to learn from him and use his laboratory. This work would never have been completed without his kind of support, continuous encouragement, and valuable guidance throughout this academic time.

Many thanks go to my colleagues in the polymer laboratories in University of Waterloo who have helped me by advising me and giving me some of their time to finish this project.

I am grateful to all of you who were enclosed me with their love and care. I thank my sisters, my brothers and my best friends for their courage and patience to overcome all the problems blended with new flavor in this short trip of our lives.

Finally, I would like to thank the Ministry of Higher Education in Kingdom of Saudi Arabia to give me the scholarship and fund me while doing Master's Degree.

Dedication

To my sweetheart,

My mother and father

My wife

Table of Contents

List of Figures

List of Tables

Nomenclature

Acronyms

CCD - Chemical Composition Distribution

CEF - Crystallization Elution Fractionation

CRYSTAF - Crystallization Elution Fractionation

^{13}C NMR - Carbon-13 nuclear magnetic resonance spectroscopy

DSC - Differential Scanning Calorimetry

FTIR - Fourier Transform Infrared Spectroscopy

GPC - Gel Permeation Chromatography

HDPE - High-density polyethylene

LDPE - Low-density polyethylene

LCBs - Long chain branches

LLDPE - Linear low-density polyethylene

MAO - Methylaluminoxane

MW - Molecular Weight

MWD - Molecular Weight Distribution

PDI - Polydispersity Index

SCBs - Short chain branches

TCB - Trichlorobenzene

TCE - Terachloroethane

TREF - Temperature Rising Elution Fractionation

TMA - Trimethylaluminum

Symbols

A - Transition metal (most commonly, Ti or Zr)

[*A*] - Concentration of monomer A

Al - co-catalyst

AlR_3 - alkylaluminum cocatalyst

A_{CH3} - Absorbance at 1378 cm^{-1} that represents the methyl branches

$Area_{CH2}$ - The area of the methylene combination band at 2019 cm^{-1}

[*B*] - Concentration of comonomer B

D_{Al} - dead polymer chain formed via a transfer to cocatalyst reaction

D_r - dead chain with a saturated end

$D_r^{=}$ - dead polymer chain containing a terminal vinyl unsaturation

E/D-n - Ethylene/1-dodecene copolymers where n is the experiment number (1, 2 … 7)

E/H-n - Ethylene/1-hexene copolymers where n is the experiment number (1, 2 … 8)

E/O-n - Ethylene/1-octene copolymers where n is the experiment number (1, 2 … 7)

H_2 - hydrogen

k_{pA} - Propagation reaction constant for monomer A

k_{pB} - Propagation reaction constant for monomer B

k_{tA} - Termination reaction constant for monomer A

k_{tB} - Termination reaction constant for monomer B

L - Ligands

M - monomer

M_n - Number average molecular weight.

M_w - Weight average molecular weight.

$[P_r^*]$ - Concentration of the active species

$P^*_{r=1}$ - growing polymer with one monomer insertion of chain length r = 1

$P^*_{r=1+n}$ - growing polymer of chain length r, where (r = 1+n) and (n) is the number of monomer insertions into the polymer chain after first insertion to the active site

P^*_r - growing polymer of chain length r

$P^*_{r\,H}$ - active site with hydrogen atom formed via chain transfer by β-hydride elimination

$P^*_{r\,Me}$ - active site with methyl group formed via chain transfer by β-methyl elimination

P^*_H - active site with hydrogen atom formed via a chain transfer to hydrogen

$P^*_{r\,M}$ - active site formed via a chain transfer to monomer

P^*_{Al} - active site with alkyl group formed via a chain transfer to cocatalyst

P_p - Probability of propagation

P_B - Probability of adding monomer B

R_p - Propagation rate

R_t - Termination rate

R - alkyl group

r_n - Number average chain length for branched copolymer

SCB/1000 C - number of short chain branches per 1000 carbons

T_m - Melting temperature

T_{peak} - Crystallization peak temperature

X - halogen atom (commonly Cl)

Chapter 1- Introduction

1.1 Introduction to Polyethylene Characterization

Polyethylene resins, such as high density polyethylene (HDPE), linear low density polyethylene (LLDPE), and low density polyethylene (LDPE), have become the most essential polymers today not only because of their low production costs, but also due to their properties that can be easily changed to achieve different required applications. The mechanical properties of polyethylene are determined by several features of its molecular structure; its chemical composition distribution (CCD) is of particular interest to this thesis.

The chemical composition distribution of ethylene/α-olefin copolymers depends on several polymerization parameters, such as catalyst type, polymerization temperature, and α-olefin/ethylene ratio. The CCD has a significant influence on the chemical, physical and thermal properties of these materials. It is, therefore, necessary to have reliable and fast quantitative analytical techniques for measuring the CCD (Soares, 2007).

Temperature rising elution fractionation (TREF) and crystallization elution fractionation (CRYSTAF) are traditional methods used to determine the CCD and crystallizability distribution of polyolefins. More recently, a new analytical technique, called crystallization elution fractionation (CEF), was developed to enhance CCD resolution and reduce analysis time (Monrabal et al., 2007).

CEF, TREF and CRYSTAF are calibrated using ethylene/α-olefin copolymer standards of narrow CCD, typically made with a single-site catalyst, to generate a plot of elution/crystallization temperature as a function of α-olefin molar fraction in the copolymer.

In this thesis, a series of homogeneous ethylene/α-olefin copolymers (1-hexene, 1-octene and 1-dodecene) with different comonomer fractions were made with a single-site catalyst under controlled conditions to produce CEF calibration standards. Their average chemical compositions were determined by ^{13}C NMR and FTIR and used to establish CEF calibration curves.

1.2 Thesis Outline

This thesis is divided into five main chapters, covering the following topics:

Chapter 1 General information on polyethylenes, analytical techniques for measuring CCD and major thesis objectives.

Chapter 2 Literature review for polyethylene synthesis and polymerization mechanism. This chapter also describes several polyolefin characterization techniques.

Chapter 3 Description of experimental procedures employed in the thesis.

Chapter 4 Discussion of experimental results, establishment of CEF calibration curves and discussion of factors that influence them.

Chapter 5 General conclusions and suggestions for future research topics.

Chapter 2 - Literature Review

2.1 Polyolefins

Polyolefins are one of the most essential polymers in modern life. It is impressive that polyolefins, made from simple monomers containing only carbon and hydrogen, can be used in a wide variety of applications in the energy industry, information technology, transportation, packaging and health care (Soares, 2007).

Polyolefins, which include large volume materials such as polyethylene and polypropylene, can be used in injection molding and extrusion applications because of their excellent rigidity, toughness, and temperature resistance, and are the most significant commodity plastics today. The large impact of polyolefins in the market is due mainly to their low production costs, their relatively low environmental impact, and their flexible and tunable physical and mechanical properties, which permit them to be used in a variety of applications (Pasch, 2001).

2.2 Polyethylene

Polyethylene is the largest volume commercial polyolefin. Polyethylene is produced by the polymerization of ethylene and other α-olefin comonomers, resulting in essentially linear chains with high molecular weight. Different polyethylene types are produced by changing the type of α-olefin comonomer used with ethylene to generate short chain branches (SCB) with distinct lengths. Polyethylene are classified according to their short and long chain branch (LCB) structure and frequency in three major types: low-density polyethylene (LDPE), linear low-density polyethylene (LLDPE), and high-density polyethylene (HDPE), as illustrated in Figure 2-1 (Soares et al., 2008).

LDPE has SCBs and LCBs, and is produced by free radical polymerization. HDPE has no, or very few, SCBs, making it more rigid and stiff than LDPE. LLDPE has a high SCB frequency, combining the toughness of LDPE with the rigidity of HDPE. Both HDPE and LLDPE are made with coordination catalysts (Soares et al., 2008).

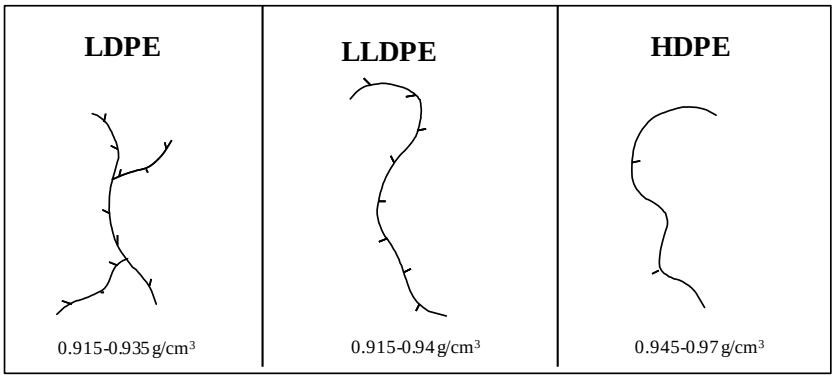

Figure 2-1. Polyethylene types: HDPE, LDPE and LLDPE (Soares et al., 2008).

2.2.1 Ethylene /α-Olefin Copolymers

Linear low density polyethylenes are materials of great commercial significance that are synthesized by the copolymerization of ethylene and different α-olefins such as 1-butene, 1-hexene, 1-octene, using several coordination catalyst types. A SCB is formed in the polymer backbone when an α-olefin is copolymerized with ethylene, as showed in Figure 2-2 (Yoon et al., 2000; Soares et al., 2008).

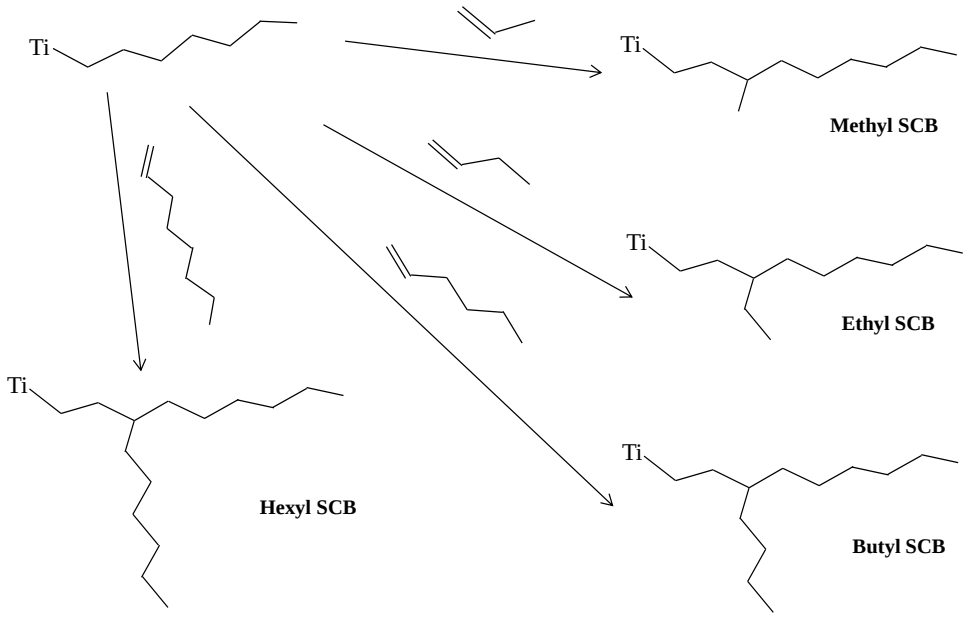

Figure 2-2. Mechanism of short chain branch (SCB) formation with coordination polymerization. The chains are shown growing on a titanium active site (Soares et al., 2008).

The inclusion of a minor SCB fraction in the backbone of these copolymers results in decreased melting points, crystallinities and densities, making them more flexible and bendable. LLDPE physical properties such as crystallinity, melting point and density depend upon structural characteristics of the copolymer chains such as molecular weight distribution and comonomer content. However, for the same comonomer mole fraction, the melting point of ethylene/α-olefin copolymers generally decrease when the short chain branches increase (methyl > ethyl > butyl > hexyl). For instance, methyl branches (shorter SCB) can be partially incorporated into the crystallites and, consequently, are less effective in decreasing the copolymer melting point. When the SCB size increases from methyl to hexyl, co-crystallization is less likely to occur (Soares et al., 2008; Mortazavi et al., 2010; Stadler et al., 2011).

2.3 Polyethylene Synthesis (Coordination Polymerization)

Most HDPE and LLDPE resins are made with multiple-site (Ziegler-Natta or Phillips catalysts) or single-site (metallocene and late transition metal) catalysts. Multiple-site catalysts make polyolefins with broad MWD and CCD, while single-site catalysts make polyolefins with narrow and uniform microstructural distributions. Table 2-1 lists the main catalyst types available commercially (Soares et al., 2008).

Table 2-1. Examples of coordination polymerization catalyst types available commercially.

Catalyst	Transition Metal	Characteristics
Metallocene	Zirconium	• Narrow molecular weight distribution • Cocatalyst required • Hydrogen as chain transfer agent
Ziegler-Natta	Titanium	• Broad molecular weight distribution • Aluminum alkyl cocatalyst required • Hydrogen is used for molecular weight control
Phillips	Chromium	• Very broad molecular weight distribution • Cocatalyst not required • Hydrogen is not used for molecular weight control

Since ethylene/α-olefin copolymers with narrow MWD and CCD are required as CEF standards, multiple-site catalysts will not be discussed any further in this chapter.

2.3.1 Single-Site Catalysts

Polyethylene properties depend on polymerization conditions and catalyst type. Metallocenes, such as the one shown in Figure 2-3, make polyethylene resins with narrow MWDs and CCDs (Kaminsky et al., 2007).

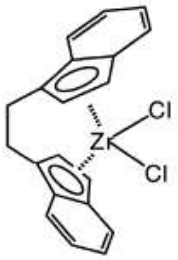

Figure 2-3. Example of a metallocene catalyst (*rac*-[En(Ind)$_2$]ZrCl$_2$).

In 1980s, the use of metallocene catalysts for the production of polyolefins with uniform properties became significant. Kaminsky and Sinn found out that metallocenes were very active for olefin polymerization when activated with methylaluminoxane (MAO), instead of trimethylaluminum (TMA) commonly used for Ziegler-Natta catalysts. MAO enhances the activity of metallocenes by a factor of about 1000 when compared to TMA. MAO is an oligomeric compound (Figure 2-4) that contains aluminum and oxygen atoms arranged alternately, albeit its precise structure (linear, cyclic, or cage) is not yet firmly established. The commercialization of metallocene polyolefins was relatively easy because polymerization processes designed for Ziegler-Natta catalysts could be adapted to work with metallocenes without major modifications (Sinn, 1995; Kaminsky, 1998; Bubeck, 2002).

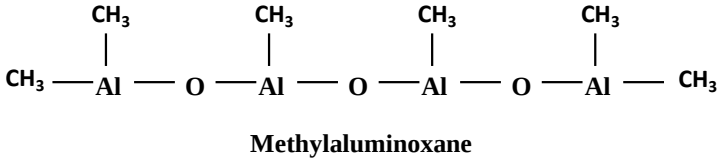

Figure 2-4. General structure of methylaluminoxane (MAO).

Metallocene catalysts are not only very active for olefin polymerization, but they also can be used to synthesize polyolefins with a degree of microstructural control which was not possible with conventional heterogeneous Ziegler-Natta and Phillips catalysts (Epacher et al., 2000; Kaminsky et al., 2001; Kaminsky et al., 2005)

2.3.2 Reaction Mechanism

The active site in coordination catalysts for olefin polymerization is a transition metal surrounded by ligands. Catalyst properties depend on the type of transition metal, geometry and electronic character of the ligands. In most cases, the active site is produced by the activation of a complex called pre-catalyst, or catalyst precursor. The creation of the active site by reaction of the pre-catalyst with an activator or cocatalyst is generally made just prior to its injection in the polymerization reactor or inside the polymerization reactor itself. The activator alkylates the pre-catalyst complex to form the active sites and stabilizes the resulting cationic active site. Because the activator works as a Lewis acid (electron acceptor) it is also used to scavenge polar impurities from the reactor. These impurities are electron donors such as oxygen, sulfur, nitrogen compounds and moisture (water, oxygen) that poison the active site. Figure 2-5 depicts a simplified chemical equation for the activation mechanism and its correspondent chemical equation. Where *A* is the transition metal (most commonly, *Ti* or *Zr*), *L* is a ligand, *X* is a halogen atom (commonly *Cl*), AlR_3 is the alkylaluminum cocatalyst, and *R* is an alkyl group (methyl, ethyl).

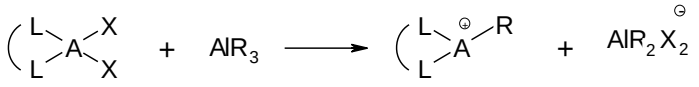

Figure 2-5. Catalyst activation by reaction of pre-catalyst and cocatalyst (Soares et al., 2008).

Coordination polymerization involves two main steps: monomer coordination to the active site and insertion into the growing polymer chain, as shown in Figure 2-6 where ($P^*_{r=1}$) is growing polymer of chain length *r*, *n* is the number of monomer, *M* is a monomer and ($P^*_{r=1+n}$) represents the growing polymer of chain length that increases. Previous to insertion, the double bond in the monomer coordinates to the active vacancy of the transition metal. After the insertion into the growing polymer

chain, another olefin monomer can coordinate to the vacant site and the process continues at a fast frequency until a chain transfer reaction takes place. In the case of copolymerization, there is a competition between comonomers to coordinate to the active sites and to be inserted into the growing polymer chains. Different comonomer coordination and insertion rates determine the final copolymer chemical composition (Soares et al., 2008).

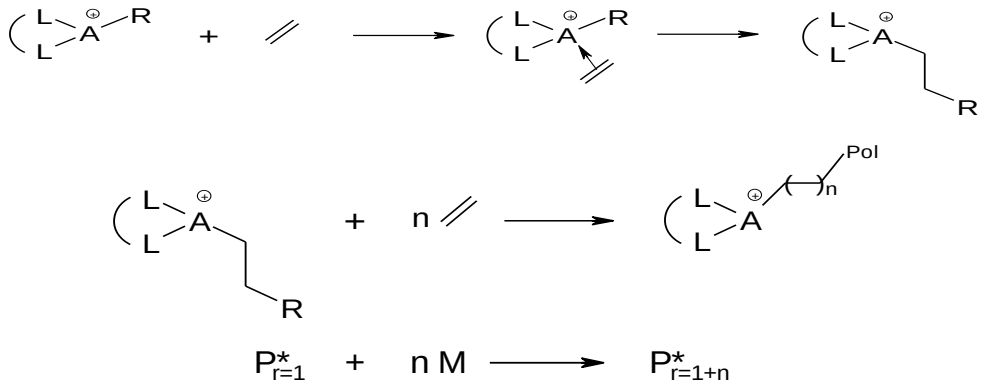

Figure 2-6. Monomer coordination and insertion (Soares et al., 2008).

Several chain transfer types are operative in coordination polymerization:

a) Transfer by β-hydride elimination.
b) Transfer by β-methyl elimination when propylene is used as monomer.
c) Transfer to monomer or comonomer.
d) Transfer to cocatalyst.
e) Transfer to chain transfer agent – commonly hydrogen.

The type of transfer reaction determines the chemical group bound to the active site and the polymer chain. Figure 2-7 illustrates these five transfer mechanisms.

a) Chain transfer by β-hydride elimination

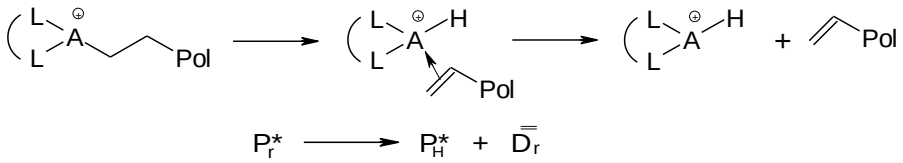

b) Chain transfer by β-methyl elimination

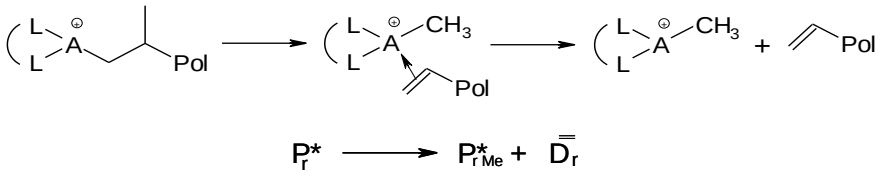

c) Chain transfer to monomer

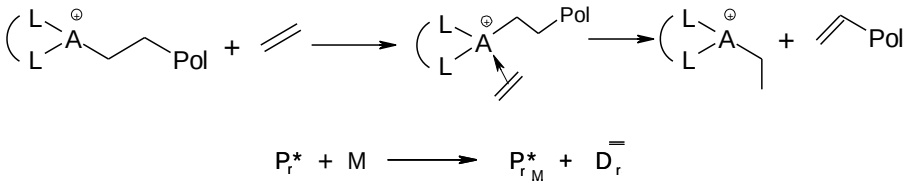

d) Chain transfer to hydrogen

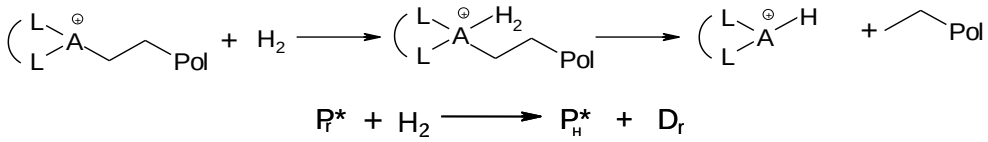

e) Chain transfer to cocatalyst

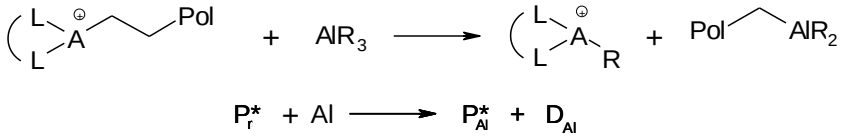

Figure 2-7. Chain transfer steps for coordination polymerization (Soares et al., 2008).

Where H_2 is hydrogen used as transfer agent, P_r^* is growing polymer of chain length *r*, $P_{r\,H}^*$ is an active site with hydrogen atom formed via chain transfer by β-hydride elimination, $P_{r\,Me}^*$ is an active site with methyl group formed via chain transfer by β-methyl elimination, P_H^* is an active site with hydrogen atom formed via a chain transfer to hydrogen, $P_{r\,M}^*$ is an active site formed via a chain transfer to monomer P_{Al}^* is an active site with alkyl group formed via a chain transfer to cocatalyst, D_{Al} is dead polymer chain formed via a transfer to cocatalyst reaction and D_r , $D_r^=$, dead polymer chain with a saturated and unsaturated end respectively.

The active site reaction with polar impurities deactivates the catalyst. Bimolecular catalyst deactivation may occur when two active sites form a stable complex that is inactive for monomer polymerization, particularly, at high catalyst concentrations. Figure 2.8 illustrates the chemical equations for this catalyst deactivation mechanism (Soares et al., 2008).

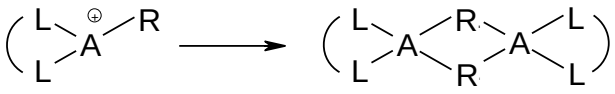

Figure 2-8 Catalyst deactivation by bimolecular reactions (Soares et al., 2008).

Some of these mechanism steps are described in the catalytic cycle shown in Figure 2-9 (Soares et al., 2008).

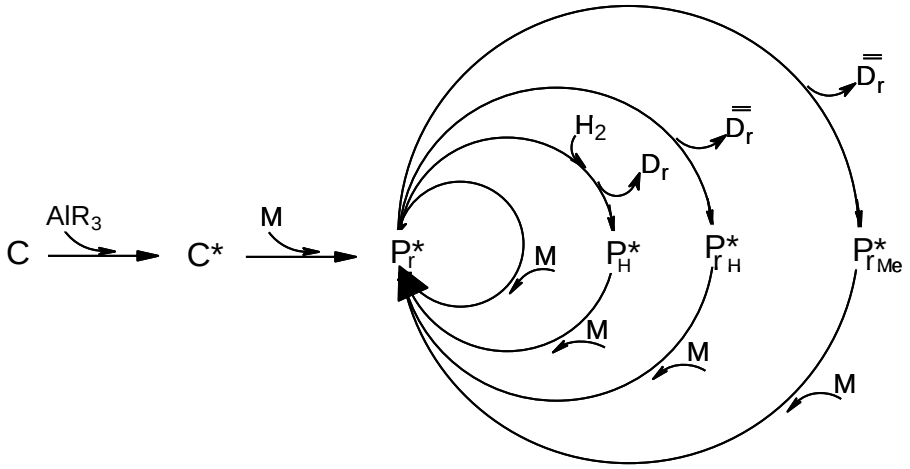

Figure 2-9. Catalytic cycle for coordination polymerization (Soares et al., 2008).

2.3.3 Homopolymer Kinetics Equations

2.3.3.1 Kinetic Equations

The accepted mechanism reaction for homopolymerization by coordination polymerization was described earlier in Chapter 2 sub-section 2.3.2. Catalyst activation with cocatalyst, catalyst initiations with monomer, chain propagation, chain transfer, and catalyst deactivation are the main steps in the coordination polymerization reaction. The catalyst activation and the Initiation with

monomer can be much fast and the concentration of active sites can be constant during the polymerization. Therefore, they do not affect the basic kinetic equations

The polymerization mechanisms can be utilized to predict the chain length of the polymer chains after termination step. The rate of propagation (R_p) is described in Figure 2-10 where the monomer insertion is repeated to form growing polymer of chain length r, ($P^*_{r=1}$) and increases its length to create ($P^*_{r=1+n}$). The rate of propagation for the monomer (R_p) is directly proportional to the concentration of the active species ($[P^*_r]$), concentration of the monomer ([M]) and the propagation kinetic constant (k_p) for the monomer (Soares, 2001).

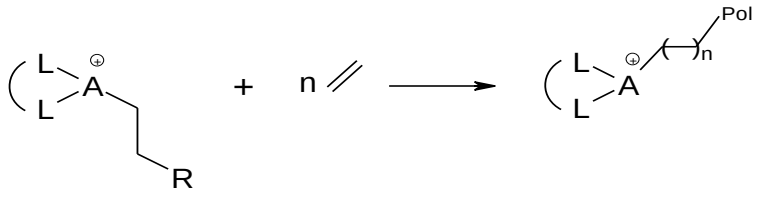

$$P^*_{r=1} + n\,M \longrightarrow P^*_{r=1+n}$$

$$R_p = k_p [P_r^*][M]$$

Figure 2-10. Propagation reaction kinetic equation for the homopolymerization (Soares et al., 2008).

Since the chain transfer reactions for termination act similar, one transfer chain reaction can be considered to simplify and understand the kinetic equations. For example, the β-hydride elimination will be only considered which is a first order reaction as shown in Figure 2-11. The hydrogen atom attached to the β-carbon in the living chain is abstracted by the active center forming a metal hydride center (P^*_H) and a dead polymer chain containing vinyl unsaturation ($D^=_r$). The polymerization reaction termination rate (R_t) is influenced by the monomer termination reaction constant (k_t) and the concentration of the active species ([P_r^*]) (Soares et al., 2008).

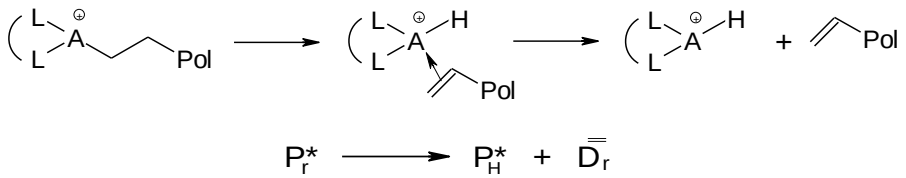

$$R_t = k_t [P_r^*]$$

Figure 2-11. Termination by transfer reaction β-hydride elimination kinetic equation for the homopolymerization (Soares et al., 2008).

2.3.3.2 Homopolymer Probabilities Calculations

The probability of propagation (P_p) and the probability of termination (P_t) are calculated using the reaction kinetic equations of the propagation and termination respectively. The number average chain length (r_n) is related to the propagation rate (R_P) and termination rate (R_t) using equation (2.1). Therefore, reducing the rate of termination of the polymerization process will lead to longer chains produced and greater number average chain length (Soares et al., 2008)

$$r_n = \frac{R_P}{R_t} \tag{2.1}$$

The chain length is related to the molecular weight by the molar mass of the monomer unit as the chain length increases the molecular weight increases too. The probability of chain propagation (P_P) is related to the number-average chain length (r_n) by following equation:

$$P_P = \frac{R_P}{R_P + R_t} = \frac{k_P[P_r^*][M]}{k_P[P_r^*][M] + k_t[P_r^*]} \tag{2.2}$$

$$P_P = \frac{R_P}{R_P + R_t} = \frac{1}{1 + \frac{R_t}{R_P}} = \frac{1}{1 + \frac{1}{r_n}} \approx 1 - \frac{1}{r_n} \tag{2.3}$$

The (P_t) is inversely proportional to the number average chain length (r_n) and is given by following equation:

$$P_t = \frac{R_t}{R_P + R_t} = \frac{k_t[P_r^*]}{k_t[P_r^*][M] + k_t[P_r^*]} \tag{2.4}$$

$$P_t = \frac{R_t}{R_P + R_t} = \frac{1}{\frac{R_P}{R_t} + 1} = \frac{1}{r_n + 1} \approx \frac{1}{r_n} \tag{2.5}$$

Therefore, the probability of propagation is expressed through the polymerization reaction kinetics and is related to the number average chain length (r_n) by using the rates of propagation and termination.

The probability of termination determines whether to add more monomer units to the growing polymer chain or to terminate the chain and store the chain length of the terminated reaction for the specific active site.

2.3.4 Copolymer Kinetics Equations

2.3.4.1 Kinetics Equations

The copolymerization reaction kinetic equations are similar to the one described for the homopolymer model except that for the copolymerization model there is monomer A and comonomer B. There is a competition between the monomer and comonomers to coordinate to the active sites and to be inserted into the growing polymer chain. The rate of propagation of monomer A (R_{pA}) and the rate of propagation of comonomer B (R_{pB}) determine the final chemical composition of the copolymer chain.

Figure 2-12 describes the rate of propagation for the copolymer model. The rate of propagation for the monomer A is influenced by the concentration of the active species ($[P_r^*]$), concentration of the monomer ($[A]$) and the propagation kinetic constant for monomer A (k_{pA}). The rate of propagation for the comonomer B is determined by the concentration of the active species ($[P_r^*]$), concentration of the comonomer B ($[B]$) and the propagation kinetic constant for comonomer B (k_{pB}).

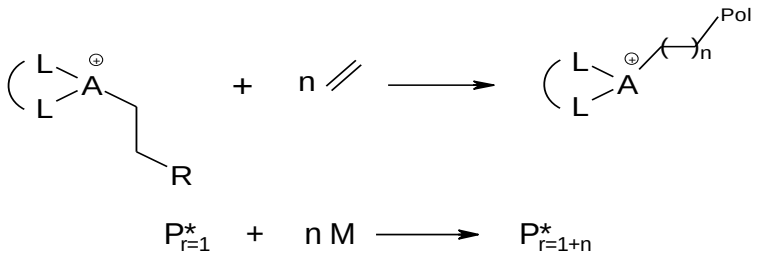

$$R_{pA} = k_{pA}[P_r^*][A]$$

$$R_{pB} = k_{pB}[P_r^*][B]$$

Figure 2-12. Propagation reaction kinetic equations for the copolymerization (Soares et al., 2008).

The termination by transfer reactions are lumped into one reaction which is described in Figure 2-13. The polymerization reaction termination rate for monomer A (R_{tA}) is determined by the termination reaction constant for monomer A (k_{tA}) and the concentration of the active species ($[P_r^*]$). The termination rate for the comonomer B (R_{tB}) is determined by the termination reaction constant for comonomer B (k_{tB}) and the concentration of the active species ($[P_r^*]$).

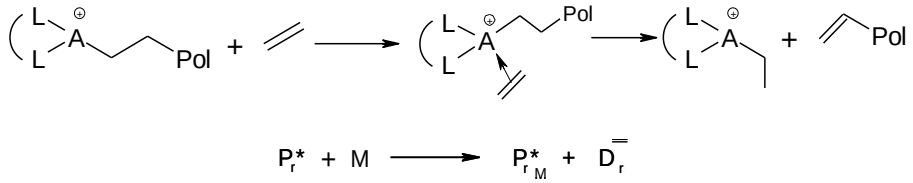

$$R_{tA} = k_{tA}[P_r^*]$$

$$R_{tB} = k_{tB}[P_r^*]$$

Figure 2-13. Termination reaction kinetic equations for the copolymerization (Soares et al., 2008).

2.3.4.2 Copolymer Probabilities Calculations

The probability of propagation (P_P) is calculated using the propagation kinetic equations for monomer A and comonomer B and the probability of termination (P_t) is calculated using the termination kinetic equations for monomer A and comonomer B. The copolymer model requires the probability of adding

comonomer B as an input to simulate a run. The probability of adding monomer B (P_B) is determined by the propagation kinetic equations for monomer A and comonomer B.

The number average chain length (r_n) is related to the propagation rate (R_p) and termination rate (R_t) of each active site using the following equation.

$$r_n = \frac{R_P}{R_t} = \frac{(R_{pA}+R_{pB})}{(R_{tA}+R_{tB})} \tag{2.6}$$

The rate of propagation for the copolymerization is represented by the sum of the rate of propagation for monomer A (R_{pA}) and the rate of propagation for comonomer B (R_{pB}). The rate of termination would be in this case represented by the sum of the rate of termination for monomer A (R_{tA}) and rate of termination for comonomer B (R_{tB}).

The chain length is related to the molecular weight by the molar mass of the monomer unit and the probability of chain propagation (P_P) is related to the number-average chain length (r_n) by:

$$P_p = \frac{R_p}{R_p+R_t} = \frac{(R_{pA}+R_{pB})}{(R_{pA}+R_{pB})+(R_{tA}+R_{tB})} = \frac{(k_{pA}[P_r^*][A]+k_{pB}[P_r^*][B])}{(k_{pA}[P_r^*][A]+k_{pB}[P_r^*][B])+(k_{tA}[P_r^*]+k_{tB}[P_r^*])} \tag{2.7}$$

$$P_p = \frac{R_p}{R_p+R_t} = \frac{1}{1+\frac{R_t}{R_p}} = \frac{1}{1+\frac{1}{r_n}} \approx 1-\frac{1}{r_n} \tag{2.8}$$

The termination rate (P_t) would be expressed by the ratio of the rate of termination to the total rates of propagation and termination. The probability of chain termination is related to the number-average chain length (r_n) by:

$$P_t = \frac{R_t}{R_p+R_t} = \frac{(R_{tA}+R_{tB})}{(R_{pA}+R_{pB})+(R_{tA}+R_{tB})} = \frac{(k_{tA}[P_r^*]+k_{tB}[P_r^*])}{(k_{pA}[P_r^*][A]+k_{pB}[P_r^*][B])+(k_{tA}[P_r^*]+k_{tB}[P_r^*])} \tag{2.9}$$

$$P_t = \frac{R_t}{R_p+R_t} = \frac{1}{1+\frac{R_p}{R_t}} = \frac{1}{r_n+1} \approx \frac{1}{r_n} \tag{2.10}$$

The probability of propagation and probability of termination are expressed through the polymerization reaction kinetics and are calculated using the rates of propagation and termination for

monomer A and comonomer B. The link between the number average chain length (r_n) and the polymerization kinetics is shown above.

2.4 Polyethylene Microstructural Characterization

The microstructure of polyethylene is defined by its distributions of molecular weight, chemical composition and long or short chain branching. Gel permeation chromatography (GPC), differential scanning calorimetry (DSC), nuclear magnetic resonance spectroscopy (NMR), Fourier-transform infrared spectroscopy (FTIR), temperature rising elution fractionation (TREF), crystallization analysis fractionation (CRYSTAF), and crystallization elution fractionation (CEF) are some of the techniques used to characterize polyolefins discussed in this section.

2.4.1 Gel Permeation Chromatography

Gel permeation chromatography is one of the most important analytical techniques to measure the molecular weight distribution of polymers. GPC is a column fractionation method in which polymer molecules are separated according to their sizes in solution. A typical gel permeation chromatographer, shown in Figure 2-14, consists of a pump to move the mobile phase (generally 1,2,4-trichlorobenzene – TCB) through a series of columns and a sample carrousel used to inject polymer sample solutions into the mobile phase. The separation takes place as the polymer molecules flow through a stationary bed of porous particles. Polymer molecules of a given size are excluded from some of the pores of the column packing, which itself has a distribution of pore sizes. Larger solute molecules can permeate a smaller proportion of the pores and thus elute from the column earlier than smaller molecules (Rudin, 1999).

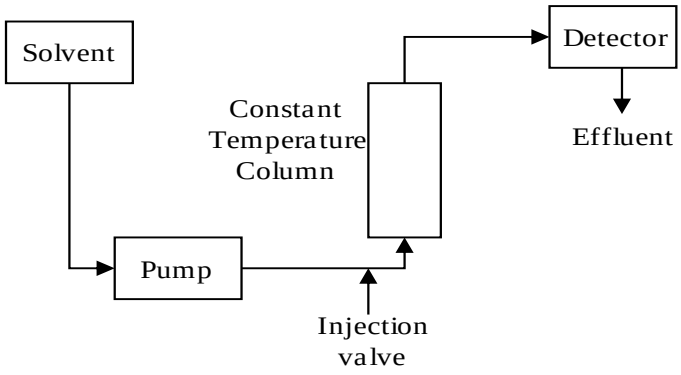

Figure 2-14. Diagram of main GPC components.

The columns are the most important part in the GPC analysis. They are filled with gel packing having different pore sizes that promote the fractionation of the polymer chains by the mechanism of size exclusion. Short chains have a small volume in solution and are able to penetrate the majority of the support pores, while long chains are able to diffuse only into the larger support pores. Consequently, chains with higher molecular weights will take shorter time to exit the column set than chains with lower molecular weights (Soares, 2004).

As a result, GPC separate polymer chains by their sizes in solution or hydrodynamic volume. The concentration of polymer, polymer type, molecular weight and branching structure, the type of solvent and temperature are factors that influence the hydrodynamic volume of polymers. The column effluent is generally monitored by at least one detector that responds to the weight concentration of the polymer in the flowing eluent. Several other detector types can be used with GPC to determine other polymer properties as a function of elution volume, such as reflective index, infrared, light scattering, and viscosity detectors (Rudin, 1999).

A series of commercially available polystyrene standards is commonly used to calibrate GPC columns. A calibration curve needs to be constructed in order to convert raw data (elution times) into the molecular weight distribution. This distribution of elution times or elution volumes can be transformed into a MWD using a calibration curve. The calibration curve is a mathematical relation between the molecular weight of a polymer standard and the time it requires to exit the GPC columns

at a given set of analytical conditions. Figure 2-15 shows a generic molecular weight calibration curve (Soares, 2004).

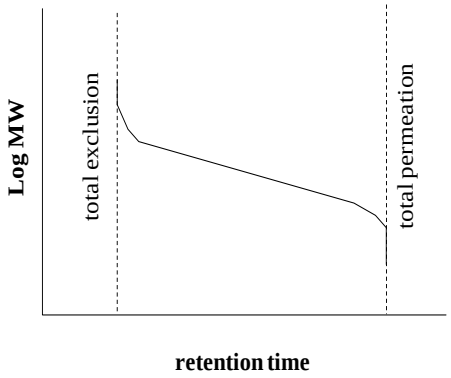

Figure 2-15. A generic GPC calibration curve.

The universal calibration curve is based on the concept that polymer molecules are separated in GPC according to their hydrodynamic volume. The universal calibration allows GPC to be calibrated for polymers for which it is difficult to obtain narrow molecular weight distribution standards. Figure 2-16 shows the standard graphical relation between the hydrodynamic volume and elution volume for polyethylene and polystyrene (Moore, 1964; Williams et al., 1968; Barlow et al., 1977).

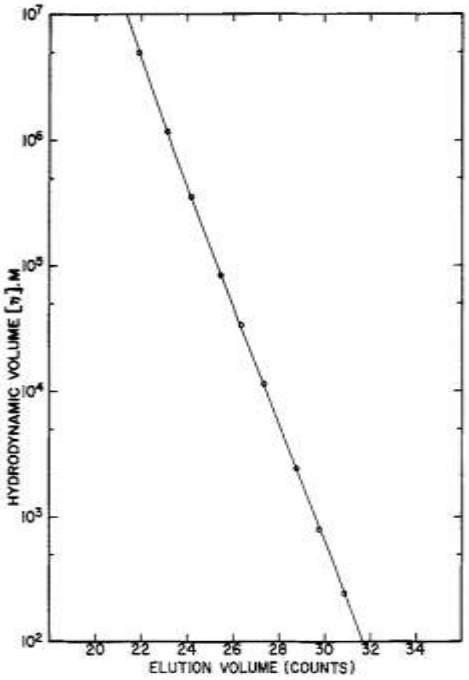

Figure 2-16. Universal GPC calibration curve illustrating that the calibration curves for polyethylene (continuous line) and polystyrene (points) are the same (Barlow et al., 1977).

The number average (M_n) and the weight average (M_w) molecular weights are commonly used to quantify the molecular weight distribution (MWD) and MWD breadth that can be determined using GPC. Polyethylenes made with a single-site-type catalyst follow the relation in equation (2.11).

$$M_w = 2 * M_n \tag{2.11}$$

The ratio of these two averages is called polydispersity index (*PDI*),

$$PDI = M_w/M_n \tag{2.12}$$

Therefore, the *PDI* of polyolefins made with single site-type catalyst is equal to two (Soares, 2004).

2.4.2 Differential Scanning Calorimetry

Differential scanning calorimetry (DSC) is the most common thermal analysis technique used for measuring changes in heat flows as function of time or temperature associated with material transitions. DSC system uses the temperature difference between the sample and a reference to calculate the heat flow. In polymeric materials, DSC is commonly used to determine several melting points, enthalpies of melting, crystallization temperatures, glass transition temperatures, and degradation temperatures. DSC can also be used to quantify the degree of crystallinity through the measurement of the enthalpy of fusion and its normalization to the enthalpy of fusion of 100 % crystalline polymer. The degree of crystallinity can be measured from the heat of fusion calculated by integrating the area under the melting peak shown in Figure 2-17 (Wunderlich, 2005; Menczel et al., 2008).

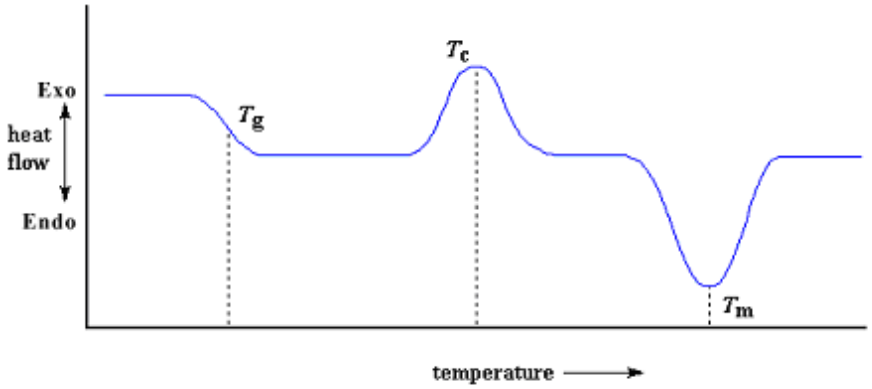

Figure 2-17. A typical polymer DSC thermogram (Menczel et al., 2008).

In a typical DSC analysis, a polymer sample is weighed (between 3-10 mg) and placed into a DSC metal sample pan. The sample pan and an empty reference pan are placed on raised platforms on the sensors as shown in Figure 2-18. The DSC cell is heated (to get the melting temperature) or cooled (to get the crystallization and glass transition temperature) at a particular controlled rate, while monitoring heat flow difference between the sample and reference pans. (Wunderlich, 2005; Menczel et al., 2008).

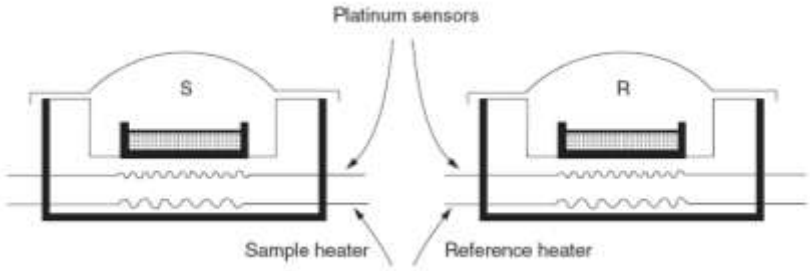

Figure 2-18. Typical power compensation sample holder with twin furnaces and sensors (Menczel et al., 2008).

DSC thermal fractionation methods are a possible alternative to analytical TREF or CRYSTAF techniques for determining the short-chain branching distribution (SCBD) and the sequence length between the chain branches in ethylene/α-olefin copolymer. The most common thermal fractionation methods based heat treatment (annealing) steps of the sample and subsequent analysis of melting point by DSC are stepwise cooling (also called stepwise crystallization or SC), and successive self-nucleation/annealing (SSA). Muller et al. (1997), Arnal et al. (2000) and Shanks et al. (2000) reported that SSA does not only provide faster analysis time than SC, but also a better separation of the segregated peaks obtained after the melting stage, particularly in the segregation of more branched molecular species at lower temperatures (Mara et al., 1994; Arnal et al., 2000; Shanks et al., 2000; Starck et al., 2002).

Sarzotti et al. (2004) analyzed the CCD of ethylene/1-hexene copolymer synthesized by single site catalyst with solution DSC as an alternative to CRYSTAF. They showed that CRYSTAF profiles analyzed at a cooling rate of 0.1 ^{o}C/min and solution DSC exotherms of samples crystallized at the cooling rate 0.01 ^{o}C/min agreed relatively well, as shown in Figure 2-19 and Figure 2-20 (Sarzotti et al., 2004)

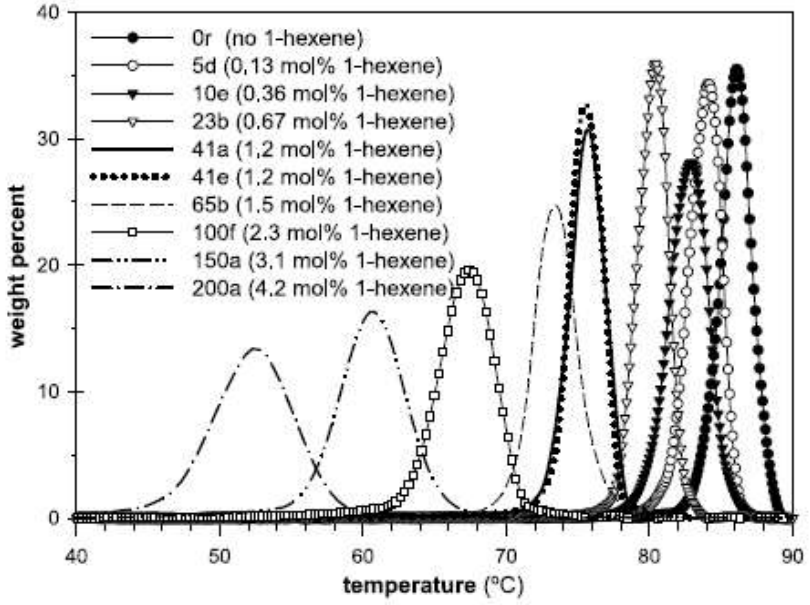

Figure 2-19. CRYSTAF profiles of ethylene/1-hexene copolymer samples obtained at a cooling rate of 0.1 °C/min.

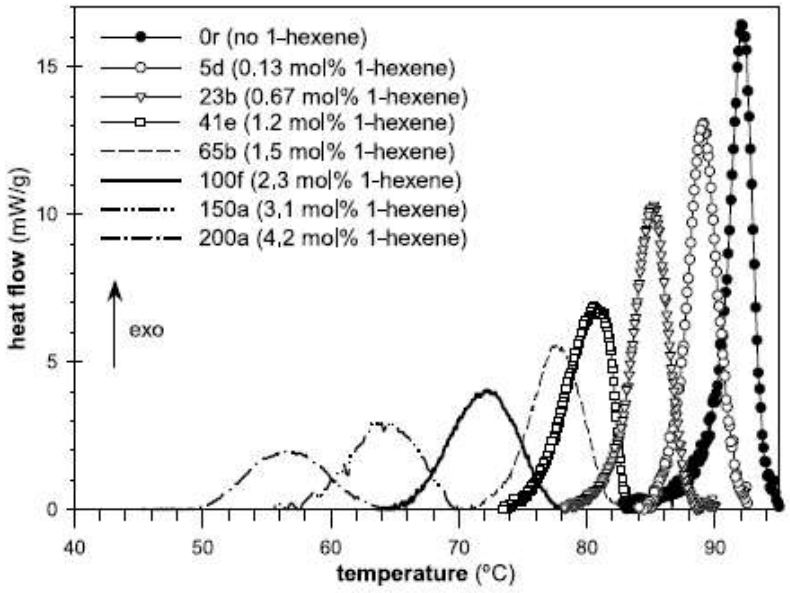

Figure 2-20. Solution DSC exotherms of ethylene/1-hexene copolymer samples obtained in TCB at a cooling rate of 0.01 °C/min.

2.4.3 Carbon-13 Nuclear Magnetic Resonance

Carbon-13 nuclear magnetic resonance is a spectrometric technique for determining chemical structures. It is a very powerful method for polymer characterization that can be used to determine and identify branching types, chain end structures, and the sequence of comonomer units in the copolymer chain without the use of a calibration curve. This technique is based upon the chemical shifts of the carbon atoms on the backbone chain attached to the branch. The chemical shift depends on the length of the branches up to five carbons (Randall, 1989; De Pooter et al., 1991; Sarzotti et al., 2002).

Slight changes in the relative position, number and type of short branches can change the final properties of polyethylene. The nomenclature displayed in Figure 2-21 were first described by Randall and by Carman and Wilkes and later extended by others. The Greek letters are used to denote the positions of a given backbone carbon atom relative to methane carbons and side-chain carbons. The format *n*B*m* denotes a branch, where *m* characterizes the length of the side chain and *n* represents the position of the carbon in question, as counted from the *end* of the side chain and also the letter *E* represents ethylene (monomer) and *H* identifies 1-hexene (comonomer) (Krimm, 1978; Randall, 1989; Seger et al., 2004).

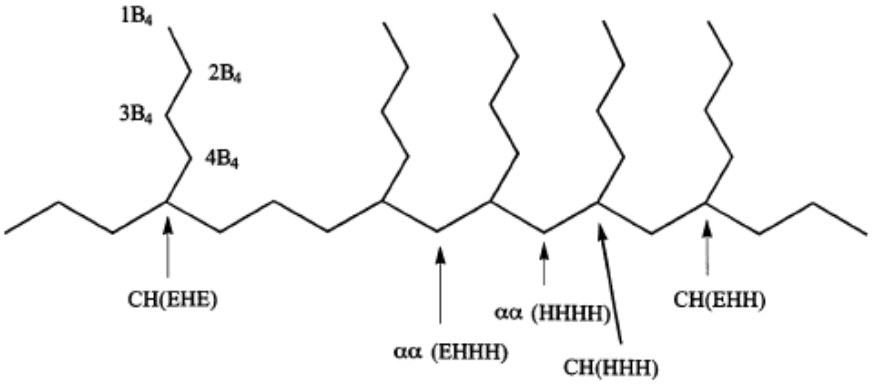

Figure 2-21. Nomenclature examples for ethylene/1-hexene copolymer substructures (Seger et al., 2004).

De Pooter et al. used the same method (which was also submitted to ASTM as Method X70-8605-2) to identify the branching structure and determine the mole fraction of comonomer in ethylene/α-olefin

copolymers by integrating all peaks in the ^{13}C NMR spectra, such as the one shown Figure 2-22 for an ethylene/1-hexene copolymer and in Figure 2-23 for an ethylene/1-octene copolymer. An accurate full scale integral is recorded from 10 to 50 ppm (the isolated methylene resonance is assigned to 30.0 ppm) (De Pooter et al., 1991; ASTM-D5017-96, 2009).

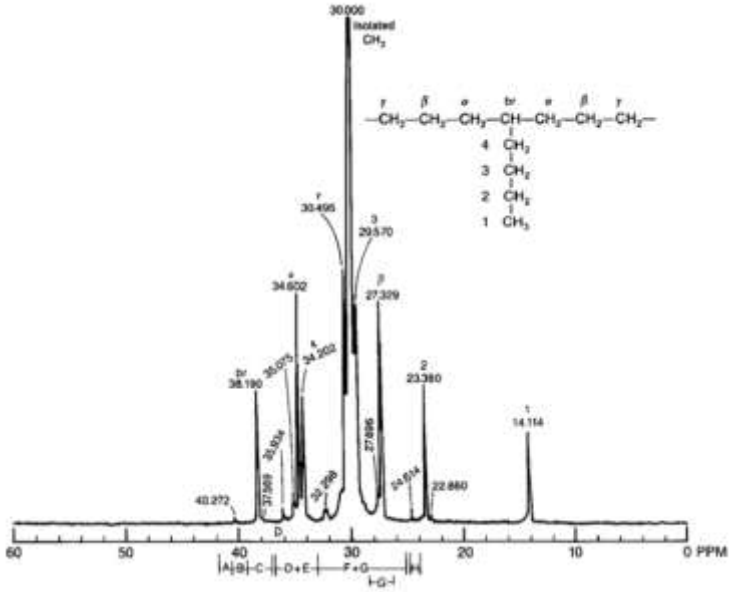

Figure 2-22. ^{13}C NMR spectrum of an ethylene/1-hexene copolymer (De Pooter et al., 1991).

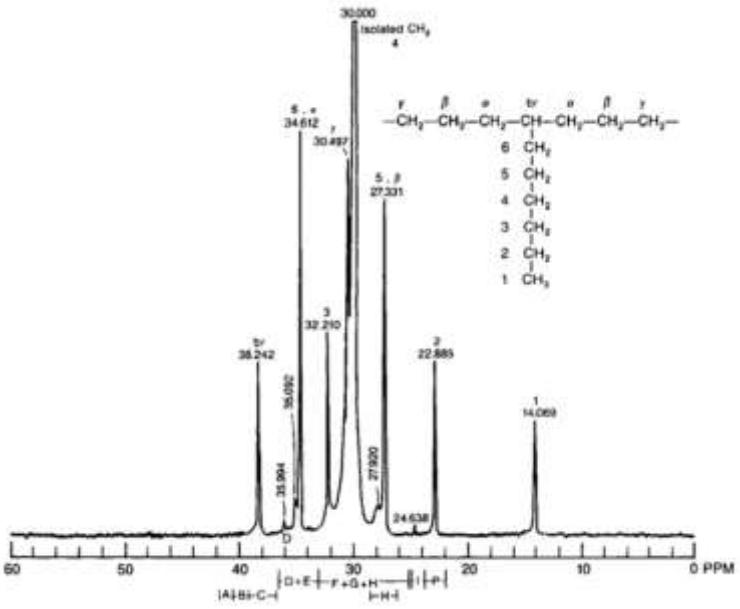

Figure 2-23. ^{13}C NMR spectrum of an ethylene/1-octene copolymer (De Pooter et al., 1991).

Table 2-2 lists the several spectral regions for ethylene/1-hexene and ethylene/1-octene copolymers.

Table 2-2. Integration limits for ethylene/α-olefin copolymers (De Pooter et al., 1991).

Copolymer	Area	Region (ppm)	Copolymer	Area	Region (ppm)
Ethylene/1-Hexene	A	41.5 to 40.5	**Ethylene/1-Octene**	A	41.5 to 40.5
	B	40.5 to 39.5		B	40.5 to 39.5
	C	39.5 to 37.0		C	39.5 to 37.0
	D	Peak at 35.8		D	Peak at 35.8
	D+E	36.8 to 33.2		D+E	36.8 to 33.2
	F+G	33.2 to 25.5		F+G+H	33.2 to 25.5
	G	28.5 to 26.5		H	28.5 to 26.5
	H	24.9 to 24.1		I	25.0 to 24.0
				P	24.0 to 22.0

After integrating the spectral regions, it is easy to determine the mole fraction by using the following equations:

Ethylene/1-hexene copolymers:

1-Hexene moles

$$H_1 = br\ carbons = \frac{(A+2C+2D)}{2} \tag{2.13}$$

$$H_2 = \ \alpha\ carbon = \frac{1.5A+2B+(C+D)-D}{3} \tag{2.14}$$

$$H' = average\ of\ Hexene\ \ moles = \frac{H_1+H_2}{2} \tag{2.15}$$

Ethylene moles

$$E' = \frac{(F+G)-(3A+3B+G+H)}{2} \tag{2.16}$$

$$mole\%\ of\ Hexene = 100 * \frac{H'}{H'+E'} \tag{2.17}$$

Ethylene/1-octene copolymers:

1-Octene moles

$$O_1 = br\ carbons = \frac{(A+2C+2D)}{2} \tag{2.18}$$

$$O_2 = \alpha\ carbon = \frac{1.5A+2B+(C+D)-D}{3} \tag{2.19}$$

$$O' = average\ of\ Octene\ \ moles = \frac{O_1+O_2}{2} \tag{2.20}$$

Ethylene moles

$$E' = \frac{(F+G+H)-(3A+3B+H+P+I)}{2} + O' \tag{2.21}$$

$$mole\%\ of\ Octene = 100 * \frac{O'}{O'+E'} \tag{2.22}$$

The comonomer mole fraction of can be converted to number of short chain branches per thousand of carbon atoms (SCD/1000 C) using the following equation (ASTM-D5017-96, 2009),

$$\mathrm{SCD/1000\ C} = \frac{1000 * (\mathrm{mole\%\ comonomer})}{2 * (\mathrm{mole\%\ ehtylene}) + \mathrm{n} * (\mathrm{mole\%\ comonomer})} \tag{2.23}$$

Where *n* is a number of carbon atoms in the comonomer.

2.4.4 Fourier Transform Infrared Specstrocopy

Fourier transform infrared spectroscopy (FTIR) is basically the absorption measurement of different infrared (IR) frequencies by a sample positioned in the path of an IR beam. The IR beam is passed through a sample and some frequencies are absorbed while other are transmitted. The resulting spectrum represents the molecular absorption and transmission and is a fingerprint of a sample with absorption peaks which correspond to the frequencies of vibrations between the bonds of the atoms

making up the material. Because each different material is a unique combination of atoms, no two compounds produce the exact same infrared spectrum (Gulmine et al., 2002).

FTIR is commonly used as a fast analytical technique to identify short chain branching type in polyethylenes in the region 1300–1400 cm^{-1} and 800–1000 cm^{-1} for unsaturated groups. Differences in the 1300–1400 cm^{-1} region have been used to identify polyethylene types (LDPE, LLDPE, and HDPE). There is an almost linear relationship between the absorptions ratio at 1369 cm^{-1} (due to methylene group C-H deformation) and 1378 cm^{-1} (due to the C-H deformation of methyl groups) and branching length in the copolymer (Blitz et al., 1994; Zhang et al., 2009).

Methyl group content in ethylene/α-olefin copolymers can be quantified with a FTIR ASTM test method. Methyl branches (with are proportional to the comonomer content in the copolymer) are quantified based on the IR absorbance at 1378 cm^{-1} (between 1330-1400 cm^{-1}) using a calibration curve. The calibration curve can be generated by plotting the ratio of the absorbance at 1378 cm^{-1} (between 1330-1400 cm^{-1}) (typically between 1330-1400 cm^{-1}) and the area of the methylene combination band at 2019 cm^{-1} (typically between 1980-2100 cm^{-1}) versus number of branches per 1000 carbons determined by ^{13}C NMR spectroscopy. Once the standard calibration curve is generated, it is easy to convert the data to comonomer content by using the following expressions (ASTM-D6645-1, 2010),

$$\mathrm{wt\%} = 100 * (\mathrm{N} * \mathrm{MW_{com}}) \,/ (\mathrm{N} * \mathrm{MW_{com}}) + \frac{(1000 - \mathrm{n} * \mathrm{N})}{2} * 28 \tag{2.24}$$

$$\mathrm{mol\%} = 100 * (\frac{Wt\%}{MW_{com}}) / (\frac{Wt\%}{MW_{com}} + \frac{100 - Wt\%}{28}) \tag{2.25}$$

Where *N* is a number of short chain branches/1000 carbons (see equation 2.23), *n* is a number of carbon atoms in the comonomer, MW_{com} is comonomer molecular weight, *Wt%* is a comonomer weight percent and *mol%* is a comonomer mole percent.

2.4.5 Crystallization Analysis Techniques

In the last three decades, temperature rising elution fractionation (TREF) and crystallization analysis fractionation (CRYSTAF) have been used to measure the comonomer distribution (short-chain branching) of polyolefins and determine their chemical composition distribution (CCD) by measuring their distribution of crystallization temperatures (CTD) (Anantawaraskul et al., 2005; Soares et al., 2008).

TREF operates in two full temperature cycles, crystallization and elution, to analyze the copolymer composition distribution. First, the sample is dissolved in a solvent at high temperature, and then the solution is introduced into a column containing an inert support, such as glass beads. This is followed by a crystallization step at a slow cooling rate. The polymer chains crystallize from lower to higher comonomer content (i.e., more crystalline chains crystallize first). TREF requires a second temperature cycle to physically separate those fractions. This is done by flowing solvent through the column while the temperature is increased. Fractions of higher crystallinity (less branch content) are dissolved as the temperature rises (Anantawaraskul et al., 2005).

In 1991, CRYSTAF was presented by Monrabal as a new analytical technique to speed up the analysis of polyolefin CCD. It shares with TREF the same fundamentals on separation based on crystallizability. However, the total fractionation process is carried out during the crystallization. In CRYSTAF, the analysis takes place in stirred crystallization vessels with no support through the crystallization process, while decreasing temperature, by observing the polymer solution concentration. CRYSTAF uses a concentration detector to analyze the solution after the filtration through an internal filter inside the vessel. In reality, the whole process is comparable to a classical stepwise fractionation by precipitation with the exception that, in this approach, no attention is paid to the precipitate but to the polymer that remains in solution. The CCD could be determined reasonably fast in a single crystallization cycle without physical separation of the fractions (Monrabal, 1996; Soares et al., 2005).

Co-crystallization is one of the main limitations of CRYSTAF analysis. Soares et al. compared two main factors regulating the co-crystallization in CRYSTAF: cooling rates and similarity of chain crystallizabilities, which is quantified by the difference between the CRYSTAF peak temperatures and comonomer type. Slow cooling rates (0.1^{o}C/min) can reduce the co-crystallization. Also,

similarity of chain crystallizabilities induces co-crystallization when the value of the differences between the CRYSTAF peak temperatures of the parent samples, ΔT_C, is very small. It seems that TREF is more suitable to have quantitative results for analyzing copolymers with complex CCDs because TREF analysis is less affected by co-crystallization for the same cooling rate (Soares et al., 2005).

In 2006, Monrabal realized that a new separation approach could be conferred based on the same principles of crystallizability and using a packed column similar to TREF, but performing the physical segregation of fractions in the crystallization step as in CRYSTAF. The new separation process is known as dynamic crystallization because cooling is performed while a small flow of solvent is passed through the column. This new analytical technique was introduced during the *First International Conference on Polyolefin Characterization* and called crystallization elution fractionation (CEF) (Monrabal et al., 2007). The next section discusses CEF and compares it to TREF and CRYSTAF.

2.5 Crystallization Elution Fractionation

2.5.1 Fractionation Procedure

Crystallization elution fractionation (CEF) is a technique used to quantify the CCD of semicrystalline polymers such as polyolefins by combining a new separation process (Dynamic Crystallization) and TREF. CEF is a faster and higher resolution alternative to previous polyolefin CCD analytical techniques such as TREF and CRYSTAF.

The CEF instrument is simple and reliable, requiring only an injection valve, a packed column, a pump, and an IR detector (Figure 2-24 shows a CEF diagram containing its main parts). The auto-sampler, attached to the CEF oven, deals with samples dissolution in 10 mL glass disposable vials. The auto-sampler dissolves the sample in 1,2,4-dichlorobenzene and loads it into the injection valve loop through a syringe dispenser (Monrabal et al., 2009).

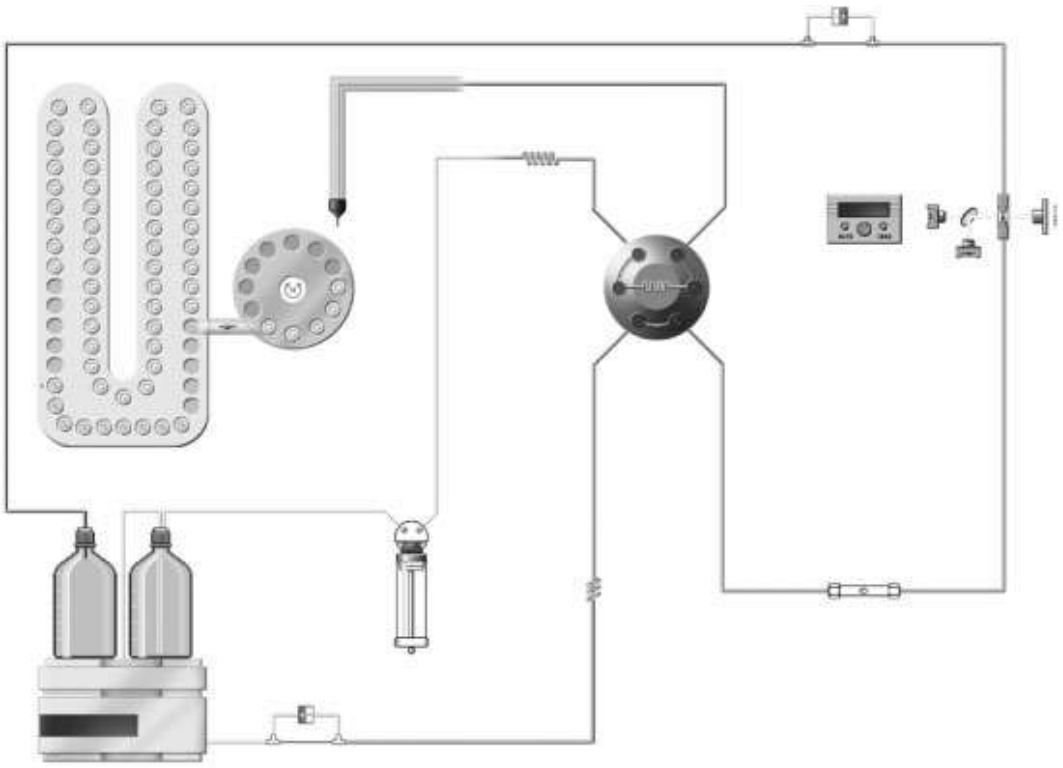

Figure 2-24. Schematic diagram for CEF (Monrabal et al., 2009).

The sample is injected with the pump flow into the column and the dynamic crystallization process begins at a given cooling rate (typically 3 ^{o}C/min) and crystallization flow rate. The flow and cooling rate are adjusted so that when the sample reaches the end of the column, the column temperature is equal to the room temperature. As the crystallization ends, the oven starts the heating program and the elution flow starts (usually at a higher rate than that for the crystallization flow). A dual wavelength infrared detector is placed at the end of the column, so that the concentration and composition of species being eluted can be measured at once. A dual capillary viscometer, as shown in the diagram, can also be added to the system to measure the composition – molar mass dependence (Monrabal et al., 2007).

A blend of three different components is represented schematically in Figure 2-25.a for TREF analysis. In the beginning of the analysis, the sample is loaded into the column, the solvent flow is stopped, and the crystallization cycle starts, causing the components to crystallize in the same

locations they were loaded as the temperature decreases. At the end of the crystallization period, the elution cycle begins by flowing solvent (Fe) through the column at increasing temperatures to elute the polymer fractions. The three components of the blend are physically separated from each other in the last cycle, as shown in Figure 2-25.a (Monrabal et al., 2007).

Figure 2-25.b represents the dynamic crystallization procedure, which is similar to TREF, but where the blend components are physically separated during crystallization by keeping a constant flow (Fc) of solvent through the column. When a component reaches its crystallization temperature, it precipitates on the support while the other components, still in solution, move along the column until they reach their own crystallization temperature. At the end of the crystallization cycle, the three components are separated inside the column according to their crystallizabilities. Once the crystallization cycle is finalized, the crystallization flow (Fc) is interrupted and the column is quickly heated for a few minutes to a temperature high enough to dissolve all components. Then, the elution cycle begins by flowing solvent through the column at increasing temperatures, as represented in Figure 2-25.b (Monrabal et al., 2007).

CEF simply combines the crystallization step in dynamic crystallization with the temperature rising elution cycle in TREF, as shown in Figure 2-25.c (Monrabal et al., 2007; Monrabal et al., 2009), by having a constant solvent flow through the column during the crystallization and elution cycles.

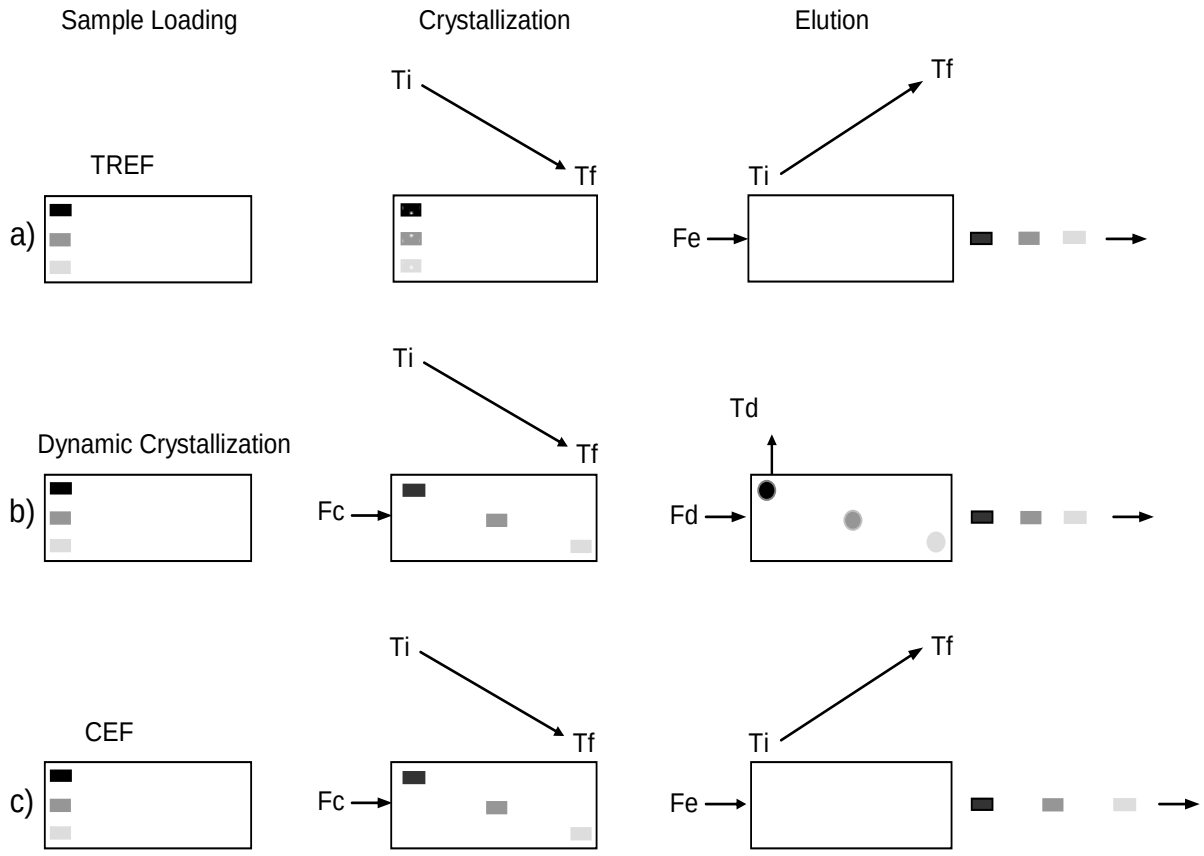

Figure 2-25. Comparison between TREF, Dynamic Crystallization and CEF operation: a) TREF, b) Dynamic Crystallization, and c) CEF (Monrabal et al., 2007; Monrabal et al., 2009).

Table 2-3 shows the main characteristics of TREF, CRYSTAF, and CEF.

Table 2-3. Main characteristics of TREF, CRYSTAF, and CEF.

TREF	Column fractionation technique
	No flow during the crystallization step
	Detection during the elution step
	Long analysis times
CRYSTAF	Batch technique
	Detection during the crystallization step
	No elution step
	Shorter analysis times than TREF
CEF	Column fractionation technique
	Flow during the crystallization step
	Detection during the elution step
	Short analysis times

2.5.2 Calibration Curve

The chemical composition distribution (CCD) of polyolefins is determined indirectly by TREF, CRYSTAF or CEF. These approaches are based on the fact that the crystallizability of polyethylenes depends on the fraction of α-olefin comonomer incorporated into the polymer chains. In CRYSTAF, chains with fewer α-olefin units crystallize at higher temperatures, while chains with a higher α-olefin fraction crystallize at lower temperatures. This information generates a CRYSTAF profile relating crystallization temperatures to the fraction of polymer that crystallizes at those temperatures. Once The CRYSTAF profile has been measured, it is converted into the CCD by means of a calibration curve relating the fraction of α-olefin in the copolymer to the crystallization temperature as conveyed in Figure 2-26. TREF calibration curves are obtained in a similar way, by relating elution temperatures to comonomer fraction in the copolymer (Soares et al., 2008).

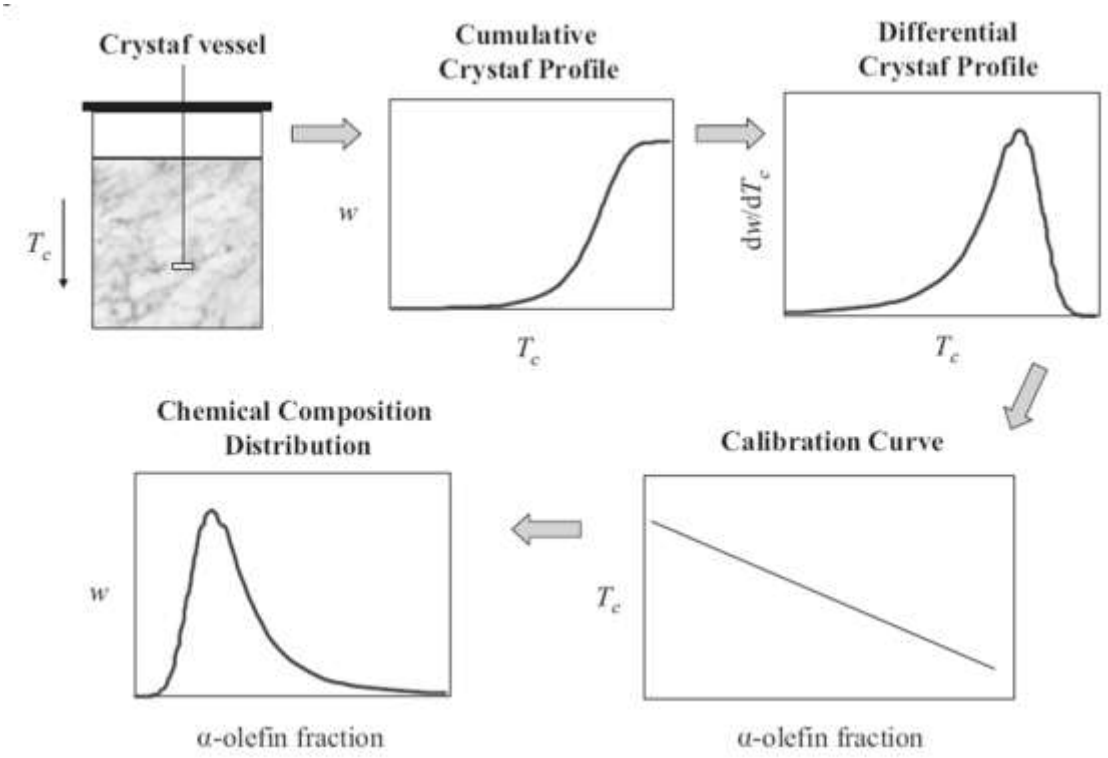

Figure 2-26. Estimation of the chemical composition distribution of a polyolefin using a CRYSTAF profile and a calibration curve (Soares et al., 2008).

Calibration curves for CRYSTAF are mathematical relationships between crystallization temperature and comonomer fraction in the polymer chain, determined by ^{13}C NMR or FTIR. Ethylene/α-olefin copolymers synthesized by single-site metallocene catalysts are useful as calibration standards for these techniques as they have narrow CCDs and cover a broad range of comonomer incorporation. Figure 2-27 shows how to generate the calibration curve. Calibration curves for CRYSTAF and TREF have been generated for ethylene/α-olefins copolymers by other researchers (Monrabal et al., 1999; Sarzotti et al., 2002; Anantawaraskul et al., 2009), but no such curves have been reported for CEF.

Samples	Comonomer Mole%
1	1.04
2	1.60
3	2.15
4	2.66
5	4.54
6	5.65
7	6.46

1) Measuring the molar fraction of comonomer of each samples using ^{13}C NMR and FTIR.

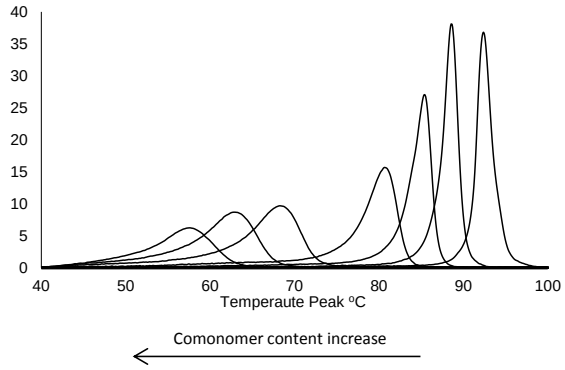

2) Analyzing the samples by CEF to determine crystallization temperature peaks

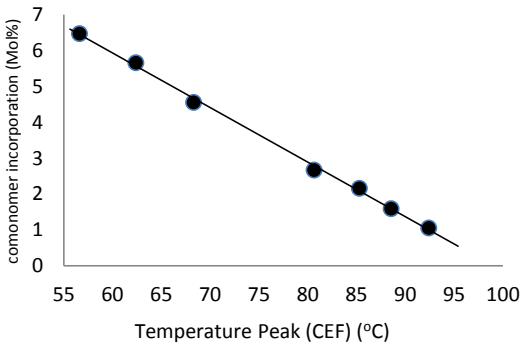

3) Plotting a linear relationship between the crystallization temperature peak and comonomer content (calibration curve)

Figure 2-27. Procedure used to generate a CEF (TREF or CRYSTAF) calibration curve.

Monrabal et al. used a series of ethylene/1-octene copolymers synthesized with a single-site catalyst to create the calibration curve illustrated in Figure 2-28. They used 17 ethylene/1-octene copolymer samples synthesized by Dow Chemical, and analyzed them by ^{13}C NMR to determine their comonomer contents and used CRYSTAF to determine the peak crystallization temperatures (Monrabal et al., 1999).

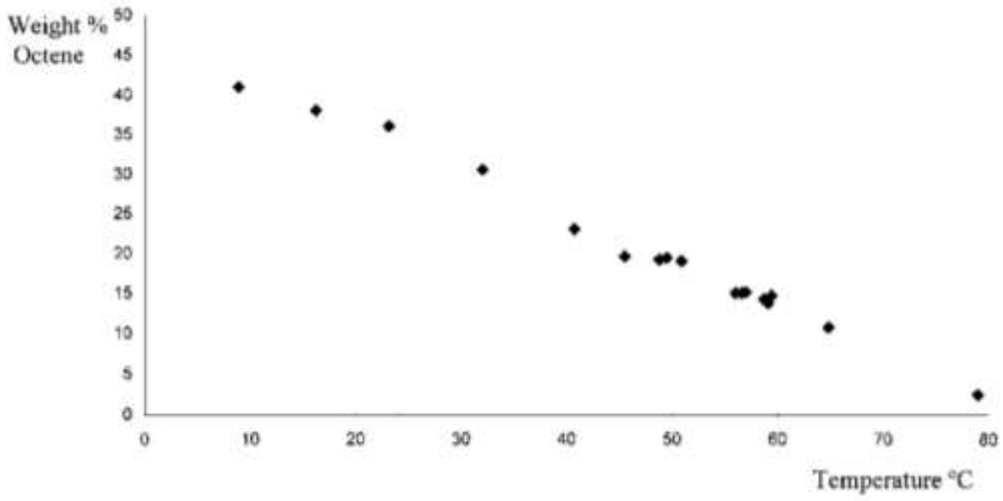

Figure 2-28. CRYSTAF Calibration curve for ethylene/1-octene copolymer using single-site (Monrabal et al., 1999).

Sarzotti et al. used nine ethylene/1-hexene copolymer samples made with a metallocene catalyst ($Et[Ind]_2ZrCl_2$/MAO) (see Figure 2-29) to obtain a linear calibration curve for CRYSTAF operated at a cooling rate of 0.1 °C/min (Figure 2-30).

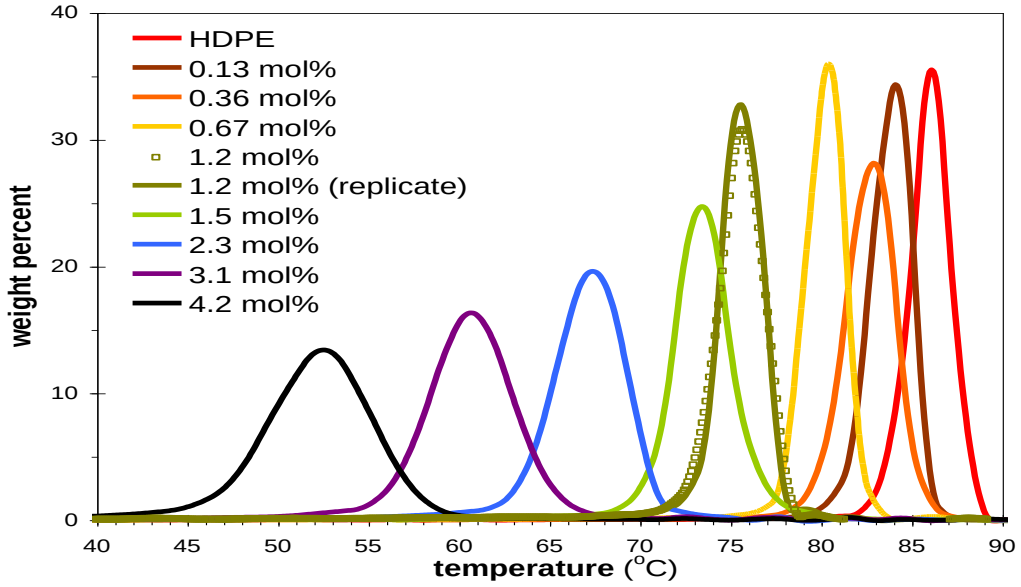

Figure 2-29. CRYSTAF profiles for ethylene/1-hexene copolymer samples showing a range of comonomer incorporation (Sarzotti et al., 2002).

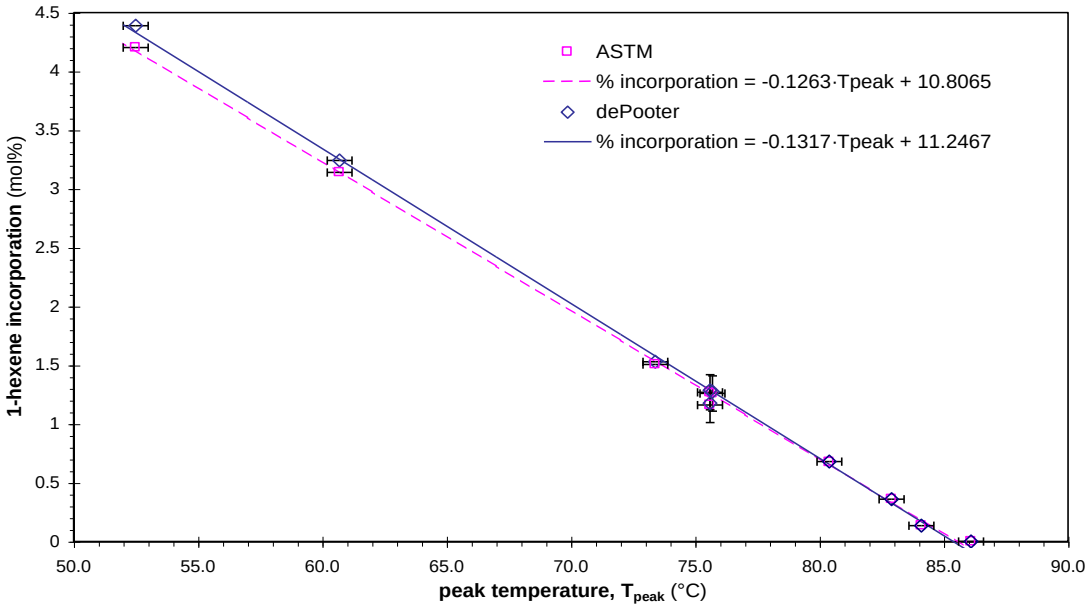

Figure 2-30. CRYSTAF calibration curves for ethylene/1-hexene copolymer (Sarzotti et al., 2002).

Chapter 3- Copolymer Synthesis and Analysis

3.1 Introduction

Three sets of compositionally homogenous ethylene/α-olefin (1-hexene, 1-octene and 1-dodecene) copolymer samples were synthesized in a stainless steel autoclave reactor operated in semi-batch mode to create CEF calibrations curves. Polymerization procedure details are given below.

Gel permeation chromatography (GPC) was used to determine molecular weight distributions (MWD) of these samples. Melting temperatures and the degrees of crystallinity for each sample were measured by DSC. FTIR and ^{13}C NMR were used to measure the average comonomer content in the copolymer. The peak elution temperature and the chemical composition distributions (CCD) of these samples were identified using crystallization elution fractionation (CEF).

3.2 Copolymer Sample Synthesis

3.2.1 Materials

All materials used in the polymerizations are listed in Table 3-1.

Table 3-1. Materials used to synthesize ethylene/α-olefin copolymers.

Material	Formula	Supplier	Grade
Ethylene	$CH_2=CH_2$	PRAXAIR	Polymer (3.0 PL-G)
1-Hexene	$CH_2=CH(CH_2)_3\ CH_3$	SIGMA-ALDRICH	97%
1-Octene	$CH_2=CH(CH_2)_5\ CH_3$	SIGMA-ALDRICH	98%
1-Dodecene	$CH_2=CH(CH_2)_9\ CH_3$	SIGMA-ALDRICH	95%
Nitrogen	N_2	PRAXAIR	5.0 UHP
Toluene	C_6H_5-CH_3	SIGMA-ALDRICH	HPLC, 99.9%
Ethanol	CH_3CH_2OH	VWR	Denatured
Methylaluminoxane (MAO)	$C_3H_9Al_3O_3X_2$	SIGMA-ALDRICH	10 wt% in Toluene
rac-Ethylene bis(indenyl)zirconium dichloride	*rac*-$Et(Ind)_2ZrCl_2$	STREM CHEMICALS	

The polymerization diluent, toluene, was distilled over a butyl lithium and metallic sodium system to remove polar impurities such as water and oxygen. Ethylene and nitrogen were flown through molecular sieves and CuO/Al_2O_3 beds to remove oxygen and water traces. The comonomers were purified by placing them over 4-Å dry molecular sieves to absorb residual moisture. A continuous flow of nitrogen was bubbled through the comonomer for 4 hours before storage. Finally, the comonomer was purged with nitrogen for 20 minutes before each polymerization. The liquid comonomers were transferred to the reactor under nitrogen pressure through a narrow cannula.

3.2.2 Catalyst Preparation

Catalyst and cocatalyst were handled under N_2 atmosphere and were stored in a glove box. Methylaluminoxane (MAO, 10 wt % in toluene) was used as received from Sigma-Aldrich. *rac*-Ethylene bis(indenyl)zirconium dichloride [*rac*-$Et(Ind)_2ZrCl_2$] was used as received from Strem Chemicals. A solution of *rac*-$Et(Ind)_2ZrCl_2$ was prepared at a concentration of 0.5 mol/g in distilled toluene before injection in the reactor. The catalyst and cocatalyst were weighed in the glove box in 20 mL vials and sealed with Teflon-lined rubber septa. Each polymerization consumed one vial of the diluted catalyst (0.3-0.45 mg, 0.15-0.225 μmol of Zr) and one vial of MAO (0.45-0.50 g, 0.3-0.45 mmol of Al), resulting in an Al/Zr ratio of about 2000.

3.2.3 Polymerization Procedure

All copolymerization experiments were synthesized in a 300 mL Parr autoclave reactor operated in semi-batch mode. Figure 3-1 shows the diagram of the polymerization reactor system. The symbols in the diagram are identified in Table 3-2.

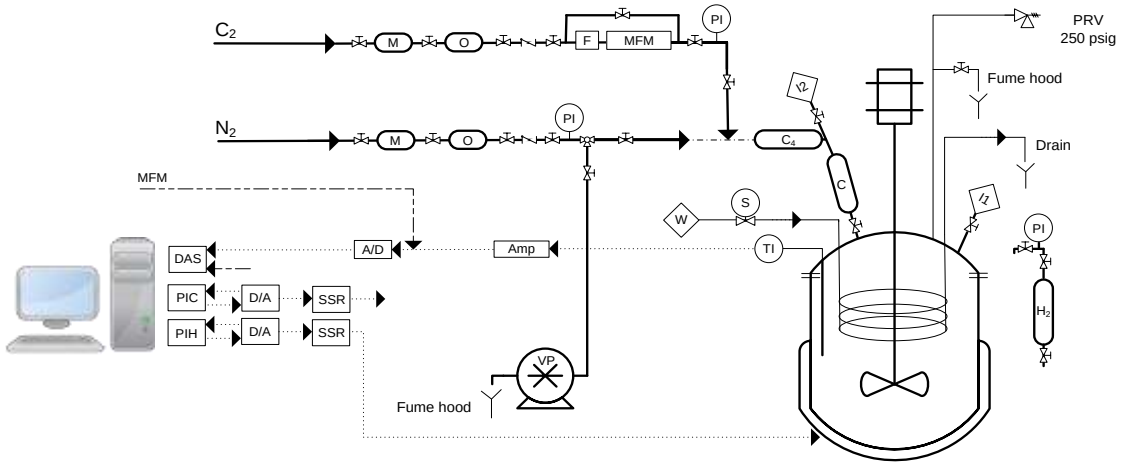

Figure 3-1. Semi-batch polymerization reactor system for ethylene/α-olefin copolymer synthesis.

Table 3-2. Definitions for Figure 3-1.

Symbol	Identification	Symbol	Identification
C_2	Ethylene supply from manifold	PI	Pressure gauge
N_2	Nitrogen supply from manifold	TI	J-type thermocouple
C_4	1-butene bomb	Amp	Signal amplifier
C	Catalyst killer bomb	A/D	Analog to digital conversion board
H_2	Hydrogen bomb	D/A	Digital to analog conversion board
M	Molecular sieves-de moisturizing	DAS	Data acquisition system
O	Deoxygenation bed (CuO on alumina)	PIC	Proportional-Integral loop for cooling
F	7 μm inlet filter	PIH	Proportional-Integral loop for heating
MFM	Mass flow meter	SSR	Solid state relay
I_1	Injection port 1	PRV	Pressure release valve
I_2	Injection port 2	VP	Vacuum pump
W	Cold water supply	Drain	Open drain for spent cooling water
S	Solenoid valve	Fume hood	Vent to fume hood

The polymerization process was divided into three main steps. In the first step, the reactor was assembled and purged under vacuum and nitrogen flow (10 psig) four times. Then, its temperature was raised to 125 ^{o}C, and finally cooled down to 30 ^{o}C. The injection points were also purged for 5 minutes with nitrogen using a narrow cannula. At this moment, the reactor was ready to receive the reactants. In the second step, the reactor temperature was raised to 50 ^{o}C. Then, distilled toluene (around 120 mL) was used to carry the required amounts of comonomer and MAO into the reactor under nitrogen pressure through the injection port 1, as shown in Figure 3-1. After that, the solution inside the reactor was saturated with ethylene to 95 psig, set by adjusting the pressure in the ethylene cylinder regulator, under a stirring rate of 500 rpm to ensure a good mixing and temperature control, while the reactor temperature was increased to 60 ^{o}C. A solution of the metallocene catalyst in toluene was introduced via injection port 2, as shown in Figure 3-1, passing a Teflon-lined sample cylinder (30 mL) with an ethylene pressure differential of 5 psig. The ethylene feed pressure was 100 psig. After checking all valve positions and sealing the injection ports, the polymerization was initiated by transferring the catalyst to the reactor. The final step included polymerization and reactor clean up. Once the polymerization started, a small exotherm was observed for about two minutes, after which the temperature became constant in the range 60 ± 0.2 ^{o}C. After about 15 to 20 minutes of polymerization, the reactor feed was closed and the polymerization ended. The heating jacket was removed and the vent was opened. After being depressurized, the reactor was opened and washed with ethanol to kill the remaining catalyst. Then, the polymer product was transferd to a beaker filled with 200 mL ethanol, stirred for approximately 4 hours, and then filtered using a Buchner funnel and Erlenmeyer flask. The resulting polymer was dried overnight in a vacuum oven.

3.3 Copolymer Analysis

3.3.1 Carbon-13 Nuclear Magnetic Resonance

A Bruker 500 MHz high resolution ^{13}C-NMR spectrometer was used to quantify the number of short chain branches per 1000 carbon atoms in the ethylene/α-olefin copolymers. Five samples were analyzed by ^{13}C-NMR and used to create a calibration curve relating the number of SCBs/1000 C to the ratio of CH_3 absorbance and CH_2 peak area determined by FTIR. A mass of 100 mg of each sample was dissolved in 1,1,2,2-terachloroethane (TCE) in a NMR tube and homogenized by heating the tube in a heating block at 120 ^{o}C for about 10 hours before the test. Typical operation conditions

were: pulse angle 90^{o}, 4000 scannings per sample, acquisition time of about 6 seconds, spin-lattice relaxation time of 10 seconds, and spectrometer reference frequency of 125 MHz. The operation temperature for the ^{13}C-NMR analysis was 120 ^{o}C. The peak calculations for number of branches were done using Equations (2.24) and (2.25), according to the methodology described in Chapter 2, Sub-Section (2.4.3).

3.3.2 Fourier Transform Infrared Specstrocopy

A Bruker FTIR Tensor 27 spectrometer was used to analyze the composition of the ethylene/α-olefin copolymer samples. Samples were prepared for FTIR spectroscopy by hot pressing about 100 mg of copolymer between polyester sheets in a mold at 145 ^{o}C. Samples were pressed for approximately 60 seconds at 1000 psi, immediately removed from the press for 30 seconds and then returned back to the press for about 60 seconds at 2000 psi to make films without bubbles. After 60 seconds, the sample was removed again from the press and air-cooled to ambient temperature. Film thicknesses, measured in three places, had thickness varying between 0.11 to 0.15 mm. Typically, 32 scans were used for spectral averaging, at a resolution of 2 cm^{-1} in the range between 400 cm^{-1} to 4000 cm^{-1}. Each spectra was used to determine the ratio of the absorbance at 1378 cm^{-1} (A_{CH3}) and the area of the combination band at 2019 cm^{-1} ($Area_{CH2}$), according to (ASTM-D6645-1, 2010) described in Chapter 2. Sub-Section (2.4.4)

3.3.3 Gel Permeation Chromatography

The molecular weight distributions of all samples were determined by high-temperature gel permeation chromatography (Polymer Char) using three linear columns (PLgel Olexis, 13 μm gel particles, 300 mm × 7.5 mm) at 140 ^{o}C. The columns were calibrated with narrow MWD polystyrene standards. The mobile phase was 1,2,4-trichlorobenzene (TCB) with flowrate of 1.0 mL/min, and the injection volume was 200 μL. The GPC chromatographer was equipped with three detectors: an IR detector to determine the concentration, a light scattering detector for absolute molecular weight determination (weight average molecular weight, M_w), and a viscometer. MWDs were calculated with the universal calibration curve and the Polymer Char software package following standard procedures.

3.3.4 Differential Scanning Calorimetry

A DSC Q2000 V24.3 (TA Instrument) was used to measure the melting temperature (T_m) and estimate the degree of crystallinity for each polymer sample. A polymer mass of 4-6 mg was weighted and prepared in a low mass pan. During DSC analysis, nitrogen at 20 ml/min was used as the purge gas. The cooling and heating rates were 10 ^{o}C/min. Two DSC heating cycles (40-160 ^{o}C) were run for each sample to erase the sample thermal history. The reported T_m values correspond to the second cycle.

3.3.5 Crystallization Elution Fractionation

All copolymer samples were analyzed using crystallization elution fractionation (Polymer Char) to identify the elution temperature peak and chemical composition distributions of each sample. From 4 to 6 mg of each sample was added to 10 mL glass disposable vials and dissolved in the autosampler in 8 mL of TCB at 145 ^{o}C for 50 minutes under continuous shaking. CEF analyses were carried out at a polymer concentration of 1.3 mg/mL and at a crystallization flow rate (Fc) of 0.04 mL/min and cooling rate of 3 ^{o}C/min until the sample reaches its crystallization (temperature became 35 ^{o}C). At the end of the crystallization period, the elution flow (Fe) began at 1.0 mL/min to elute the polymer sample precipitated into the column while the temperature increasing upto140 ^{o}C at a heating rate of 3^{o}C/min. These CEF analytical conditions were chosen because they are standard conditions recommended by Polymer Char.

Chapter 4- Results and Discussion

4.1 Introduction

The reaction conditions for ethylene polymerization performed with various amount of 1-hexene, 1-octene and 1-dodecene are shown in Table 4-1, Table 4-2, and Table 4-3, respectively. For all experiments, the ethylene pressure was kept at 100 psi, the toluene volume was 150 mL, the cocatalyst/catalyst ratio was 2000, and the reaction temperature was 60 ^{o}C. The sample ID's follow the convention: the first letter identifies the (E = ethylene), the second letter the comonomer (H = 1-Hexene, O = 1-Octene, and D = 1-Dodecene), and the number indicates the experiment number.

Table 4-1. Ethylene/1-hexene copolymerization conditions.

Sample ID	Catalyst (Zr) (μmol)	1-Hexene (mL)	1-Hexene concentration (mol/L)
E/H-1	0.23	1.19	0.008
E/H-2	0.15	2.50	0.016
E/H-3	0.15	5.36	0.036
E/H-4	0.15	6.27	0.042
E/H-5	0.23	12.60	0.084
E/H-6	0.15	18.62	0.124
E/H-7	0.15	23.30	0.155
E/H-8	0.15	24.92	0.166

Table 4-2. Ethylene/1-octene copolymerization conditions.

Sample ID	Catalyst (Zr) (μmol)	1-Octene (mL)	1-Octene concentration (mol/L)
E/O-1	0.23	1.07	0.007
E/O-2	0.15	2.34	0.015
E/O-3	0.15	7.57	0.050
E/O-4	0.15	11.26	0.075
E/O-5	0.15	16.85	0.112
E/O-6	0.23	21.08	0.140
E/O-7	0.23	31.61	0.210

Table 4-3. Ethylene/1-octene copolymerization conditions.

Sample ID	Catalyst (Zr) (μmol)	1-Dodecene (mL)	1-Dodecene concentration (mol/L)
E/D-1	0.23	0.61	0.004
E/D-2	0.15	2.44	0.016
E/D-3	0.15	4.41	0.029
E/D-4	0.23	9.89	0.066
E/D-5	0.15	15.20	0.101
E/D-6	0.15	22.53	0.15
E/D-7	0.15	35.07	0.23

4.2 Copolymer Characterization Analysis

4.2.1 Compostion Characterization by CEF

The crystallization peak temperature of the ethylene/α-olefin copolymers are shown in Table 4-4, Table 4-5, and Table 4-6. The CEF profiles of ethylene/1-hexene, ethylene/1-octene, and ethylene/1-dodecene copolymers are shown in Figure 4-1, Figure 4-2, and Figure 4-3, respectively. All profiles are narrow, confirming that the samples have uniform chemical composition distributions, characteristic of copolymers synthesized with single-site catalysts. Because of the chemical composition distributions are unimodal and approximately symmetrical, the peak temperature values are a good indicator of their average comonomer incorporations.

The CEF profiles show that as the comonomer content in the copolymer increases, the CEF curves shift to lower elution temperatures, as expected, since the presence of short chain branches (SCB) formed via comonomer incorporation disrupt the crystallizability of the ethylene segments in the polymer chains.

Table 4-4. Characterization data for ethylene/1-hexene copolymers.

Sample ID	E/H-1	E/H-2	E/H-3	E/H-4	E/H-5	E/H-6	E/H-7	E/H-8
T_{peak} (°C)	94.59	92.41	88.55	85.30	80.66	68.31	62.40	56.62
T_m (°C)	128.18	123.39	118.60	113.93	109.52	100.45	94.35	89.73
Crystallinity %	65.30	61.82	47.73	41.36	28.02	22.57	12.87	7.30
SCB/1000 C	1.57	5.14	7.71	10.33	12.65	20.85	25.39	28.62
$A_{CH3}/Area_{CH2}$	0.02	0.06	0.08	0.10	0.13	0.20	0.24	0.27
1-Hexene wt%	0.94	3.09	4.63	6.21	7.60	12.53	15.26	17.20
1-Hexene mol%	0.32	1.05	1.59	2.15	2.67	4.55	5.65	6.46
M_w (g/mol)	88,696	81,691	77,031	76,931	69,667	63,863	60,800	61,273
M_n (g/mol)	39,393	37,444	35,270	35,511	33,323	31,253	29,495	29,413
PDI	2.25	2.18	2.18	2.17	2.09	2.04	2.06	2.08

Table 4-5. Characterization data for ethylene/1-octene copolymers.

Sample ID	E/O-1	E/O-2	E/O-3	E/O-4	E/O-5	E/O-6	E/O-7
T_{peak} (°C)	96.36	92.35	86.18	82.85	75.75	66.42	64.47
T_m (°C)	128.58	123.46	114.49	112.41	107.10	98.71	96.48
Crystallinity %	81.07	59.16	39.72	35.71	25.62	16.57	13.51
SCB/1000 C	2.04	3.97	8.51	9.54	13.64	19.11	20.80
$A_{CH3}/Area_{CH2}$	0.03	0.05	0.09	0.10	0.14	0.19	0.20
1-Octene wt%	1.64	3.18	6.82	7.65	10.93	15.31	16.67
1-Octene mol%	0.41	0.81	1.79	2.02	2.97	4.32	4.75
M_w (g/mol)	83,502	81,093	78,487	69,139	68,392	65,696	63,972
M_n (g/mol)	44,226	38,075	36,839	35,349	32,897	32,163	31,826
PDI	1.89	2.13	2.13	1.96	2.07	2.04	2.01

Table 4-6. Characterization data for ethylene/1-dodecene copolymers.

Sample ID	E/D-1	E/D-2	E/D-3	E/D-4	E/D-5	E/D-6	E/D-7
T_{peak} (°C)	97.35	95.41	91.29	89.17	84.77	79.64	69.80
T_m (°C)	129.70	126.64	122.18	118.77	114.75	111.12	101.52
Crystallinity %	85.31	70.42	60.46	55.27	41.33	33.43	20.09
SCB/1000 C	1.24	2.64	4.33	6.12	9.11	11.07	16.59
$A_{CH3}/Area_{CH2}$	0.02	0.03	0.05	0.07	0.09	0.11	0.16
1-Dodecene wt%	1.49	3.18	5.20	7.36	10.95	13.30	19.93
1-Dodecene mol%	0.25	0.54	0.90	1.30	2.00	2.49	3.98
M_w (g/mol)	87,737	89,688	88,127	83,308	75,091	70,378	68,883
M_n (g/mol)	42,045	39,905	39,231	37,262	34,439	34,877	32,360
PDI	2.09	2.24	2.24	2.23	2.18	2.02	2.13

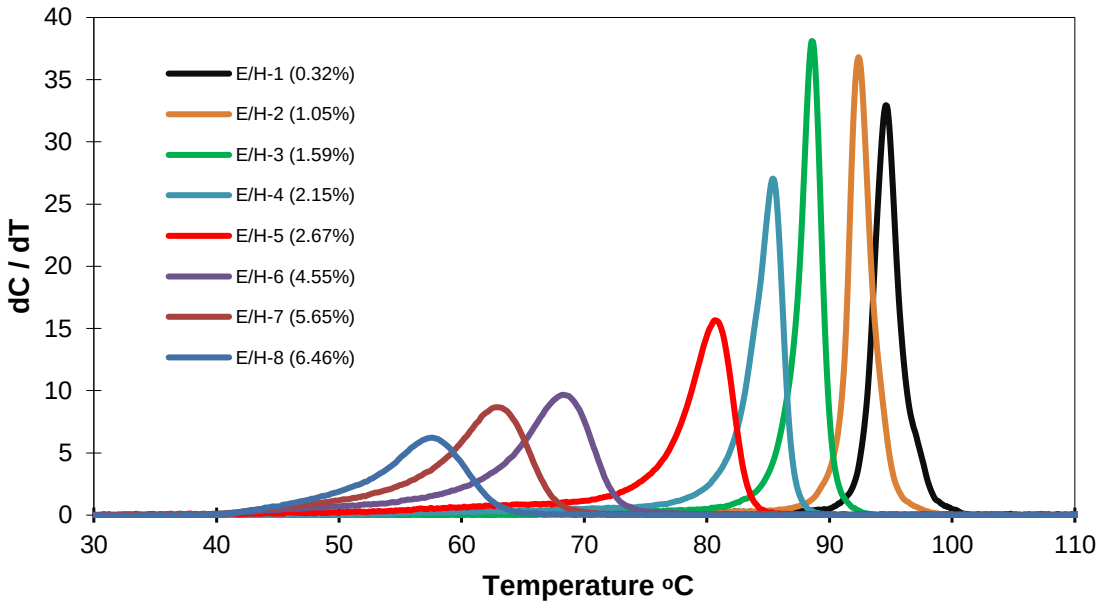

Figure 4-1. CEF profiles for ethylene/1-hexene copolymers.

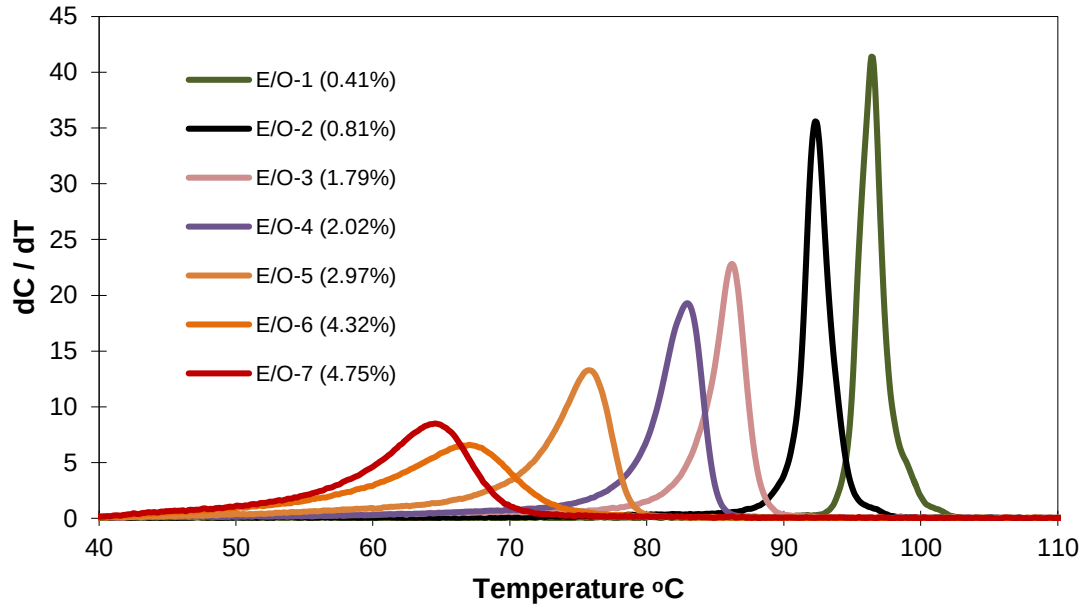

Figure 4-2. CEF profiles of ethylene/1-octene copolymer.

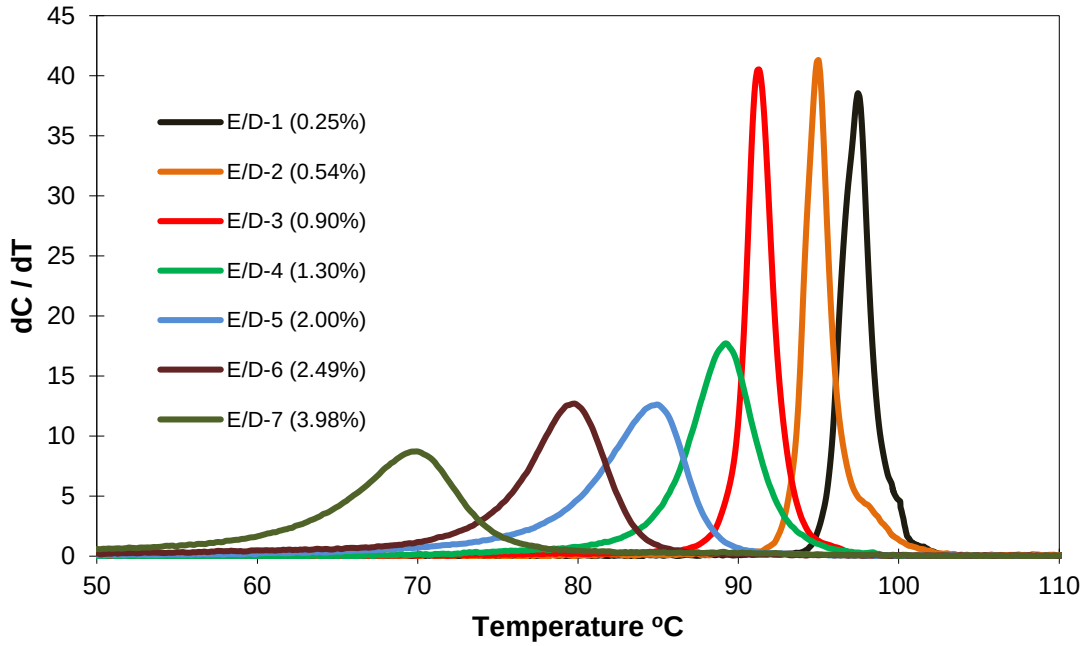

Figure 4-3. CEF profiles of ethylene/1-dodecene copolymer.

4.2.2 Compostion Characterization by ^{13}C NMR

Four ethylene/1-hexene copolymers and one ethylene/1-octene copolymer were randomly chosen and analyzed by ^{13}C NMR to establish a FTIR calibration curve for all copolymers investigated in this thesis. A typical ^{13}C NMR spectrum for an ethylene/1-octene copolymer is shown in Figure 4-4 (see appendix A for the ^{13}C NMR spectra of all samples).

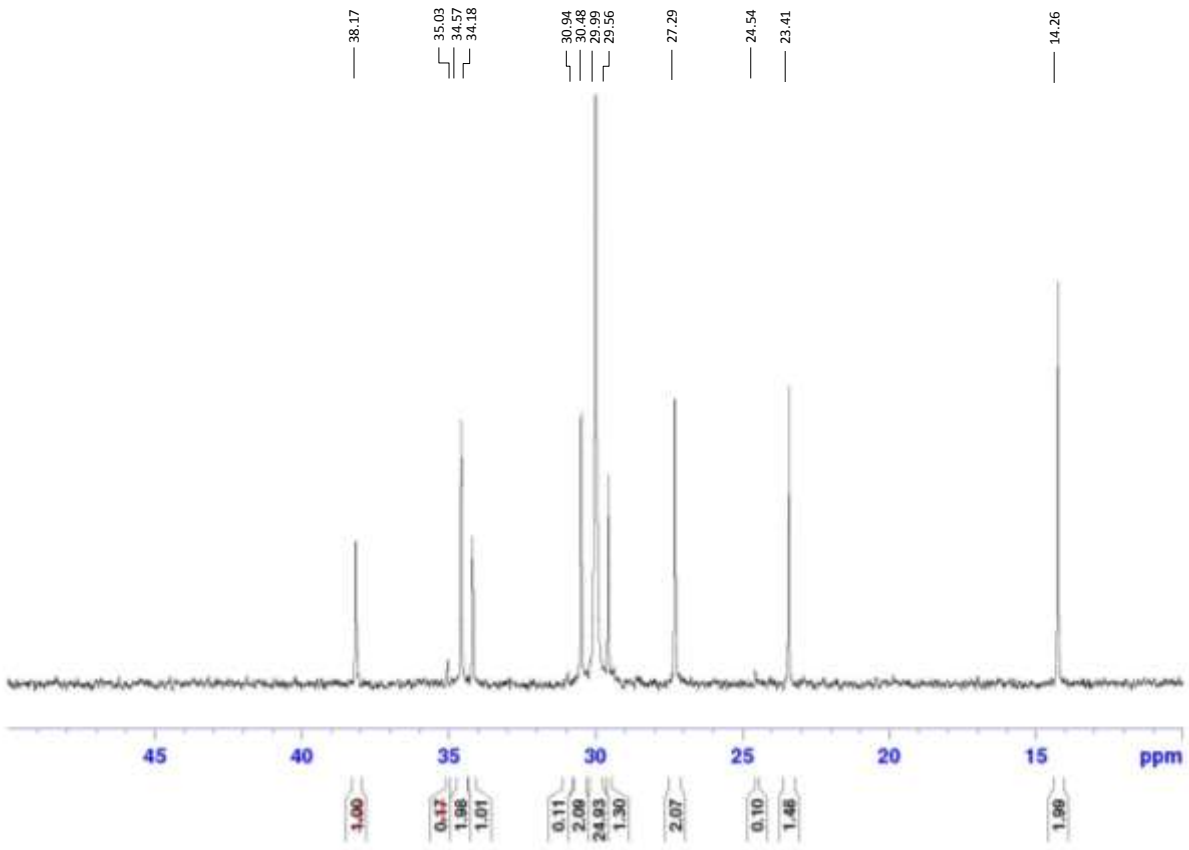

Figure 4-4. ^{13}C NMR spectrum of sample E/H-8 with selected peak assignments and peak areas.

The determinations of the molar fractions for these samples were carried out according to ASTM Method X70-8605-2. Table 4-7 and Table 4-8 show the integration limits and comonomer molar fraction of these five samples. Once the molar fraction of the comonomer is known, the number of short chain branches per 1000 carbons (SCB/1000 C) can be calculated using Equation (2.23). In addition, the ratio of the absorbance CH_3 (A_{CH3}) and the area of CH_2 ($Area_{CH2}$) were calculated for these five samples using FTIR to establish the FTIR calibration curve.

Table 4-7. Integration limits and ethylene/1-hexene molar fractions.

Area	Region ppm	E/H-1	E/H-5	E/H-6	E/H-8
A	41.5-40.5	0	0	0	0
B	40.5-39.5	0	0	0	0
C	39.5-37.0	1	1	1	1
D	Peak at 35.8	0	0.05	0.11	0.16
D+E	36.8-33.2	3.08	3.28	2.94	3.010
F+G	33.2-25.5	460.70	86.36	42.62	30.49
G	28.5-26.5	1.97	2.07	1.85	2.06
H	24.9-24.1	0	0	0	0.10
	H_1	1.02	1.07	0.94	0.94
	H_2	1.00	1.05	1.11	1.16
	H'	1.01	1.06	1.02	1.05
	E'	230.37	43.20	21.41	15.21
1-Hexene mole fraction		0.36	2.40	4.58	6.49
SCB/1000 C		2.17	11.46	21.01	28.74
A_{CH3} / $Area_{CH2}$		0.0243	0.1263	0.2017	0.2732

Table 4-8. Integration limits and ethylene/1-octene molar fraction .

Area	Region ppm	E/O-4
A	41.5-40.5	0
B	40.5-39.5	0
C	39.5-37.0	1
D	Peak at 35.8	0.1
D+E	36.8-33.2	3.195
F+G+H	33.2-25.5	105.486
H	28.5-26.5	3.258
I	25.0-24.0	0
P	24.0-22.0	1.725
	O_1	1.1
	O_2	1.032
	O'	1.066
	E'	51.317
	1-Octene mole fraction	2.035
	SCB/1000 C	9.588
	$A_{CH3}/Area_{CH2}$	0.0977

Figure 4-5 shows that the relation between $A_{CH3}/Area_{CH2}$ and SCB/1000 C is linear. Observing the relatively high coefficient of correlation (0.9958), it can be said that the calculated linear relationship is strongly representative of the collected results. The final calibration curve is given by the expression,

$$(SCB/1000\ C) = (A_{CH3}/Area_{CH2} - 0.0099)/0.0092 \quad (4.1)$$

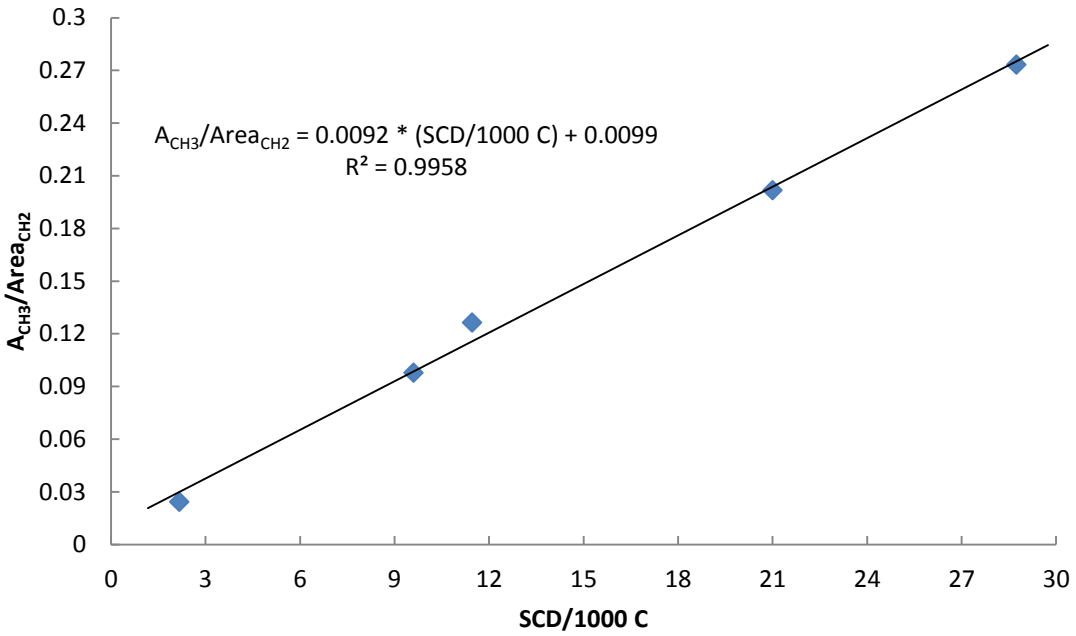

Figure 4-5. FTIR calibration curve.

4.2.3 Compostion Characterization by FTIR

All ethylene/α-olefin copolymer samples were analyzed using FTIR, following the procedure illustrated in Figure 4-6. The absorbance height value at 1378 cm^{-1}, representing methyl branches (A_{CH3}) (Figure 4-6.b) was measured for each sample, as well as the area of the methylene combination band at 2019 cm^{-1} ($Area_{CH2}$) (Figure 4-6.c), to calculate the ratios shown in Table 4-9. Equation (4.1) was used to calculate the SCB/1000 C, and the comonomer mole fractions were calculated using Equations (2.24) and (2.25) (see Chapter 2 section 2.4.4). These calculations are presented in Table 4-4, Table 4-5 and Table 4-6 for ethylene/1-hexene, ethylene/1-octene, and ethylene/1-dodecene copolymers, respectively.

As expected, A_{CH3} height value increases with increasing the comonomer contents in the ethylene/α-olefin copolymers, which leads to increase the methyl branches, as shown in Figure 4-7.

Table 4-9. FTIR data for ethylene/α-olefin copolymers.

Sample ID	$Area_{CH2}$	A_{CH3}	$A_{CH3}/Area_{CH2}$
E/H-1	2.122	0.052	0.02
E/H-2	1.926	0.110	0.06
E/H-3	1.257	0.102	0.08
E/H-4	1.180	0.124	0.10
E/H-5	1.172	0.148	0.13
E/H-6	1.133	0.229	0.20
E/H-7	0.795	0.194	0.24
E/H-8	0.636	0.174	0.27
E/O-1	1.959	0.056	0.03
E/O-2	1.706	0.079	0.05
E/O-3	1.065	0.094	0.09
E/O-4	1.377	0.135	0.10
E/O-5	1.052	0.142	0.14
E/O-6	1.325	0.246	0.19
E/O-7	0.786	0.158	0.20
E/D-1	0.923	0.020	0.02
E/D-2	0.793	0.027	0.03
E/D-3	0.818	0.044	0.05
E/D-4	0.922	0.055	0.06
E/D-5	1.052	0.091	0.09
E/D-6	1.457	0.149	0.10
E/D-7	1.546	0.251	0.16

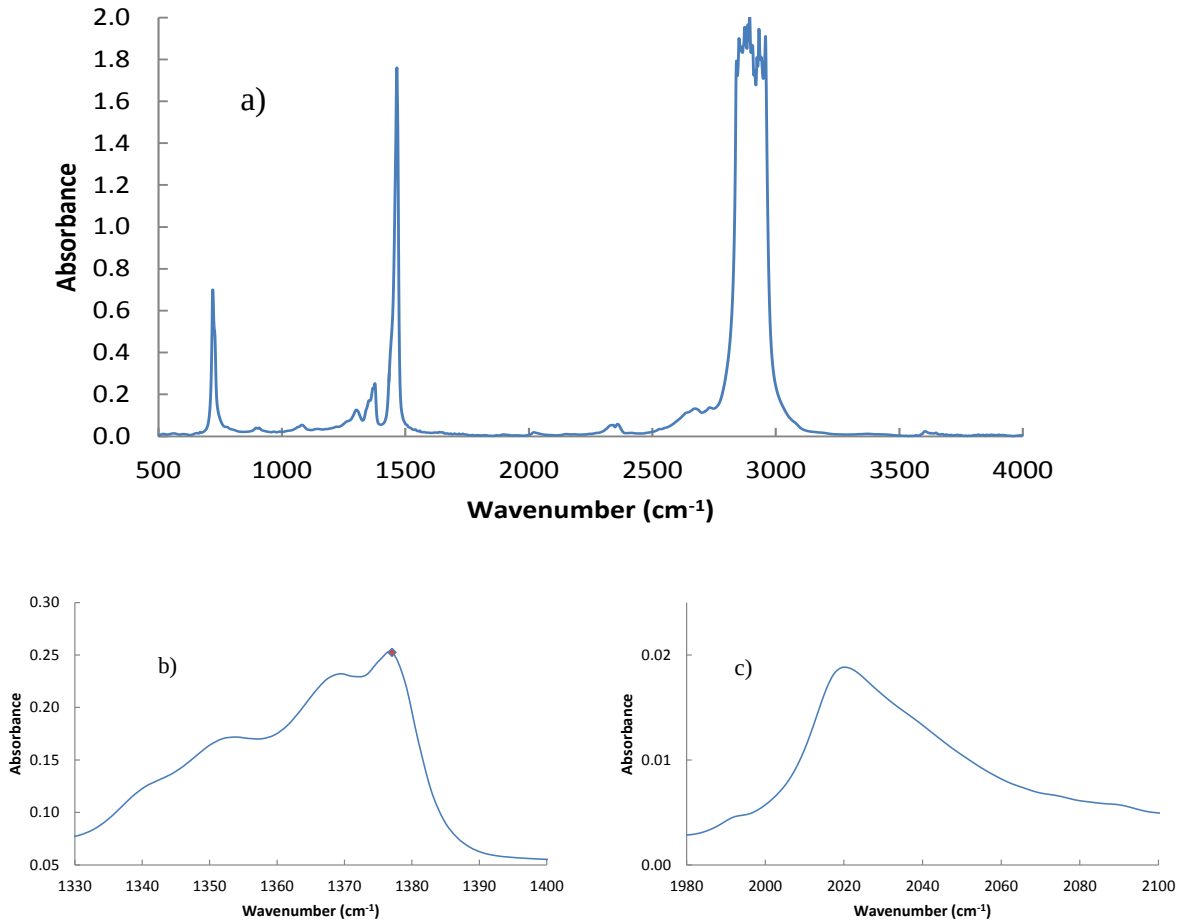

Figure 4-6. FTIR spectrum of poly(ethylene-co-1-hexene) containing 6.46% of comonomer: a) spectrum showing the extent range (500-4000), b) spectrum showing the range (1330-1400 cm^{-1}) to measure (A_{CH3}), and c) spectrum showing the range (1980-2100 cm^{-1}) to measure ($Area_{CH2}$).

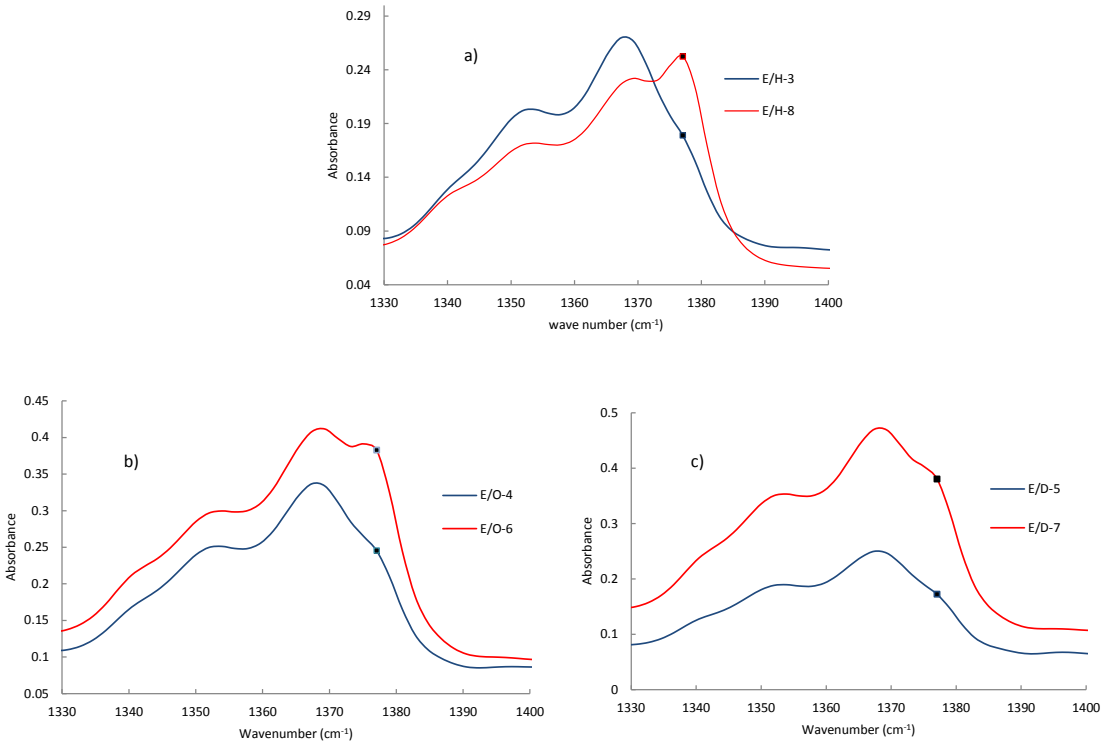

Figure 4-7. A_{CH3} height values for ethylene/α-olefin copolymers with various comonomer contents: a) E/H-3 compared with E/H-8, b) E/O-4 compared with E/O-6, and c) E/D-5 compared with E/D/-7.

4.2.4 Molecular Weight Characterization

Ethylene/α-olefin copolymer samples were analyzed with high-temperature GPC. Molecular weight averages are presented in Table 4-4, Table 4-5 and Table 4-6. All copolymers have polydispersities close to 2.0, which is theoretically expected for polymers made with single-site catalysts. Figure 4-8, Figure 4-9, and Figure 4-10 show the MWDs for ethylene/1-hexene, ethylene/1-octene, and ethylene/1-dodecene copolymers respectively.

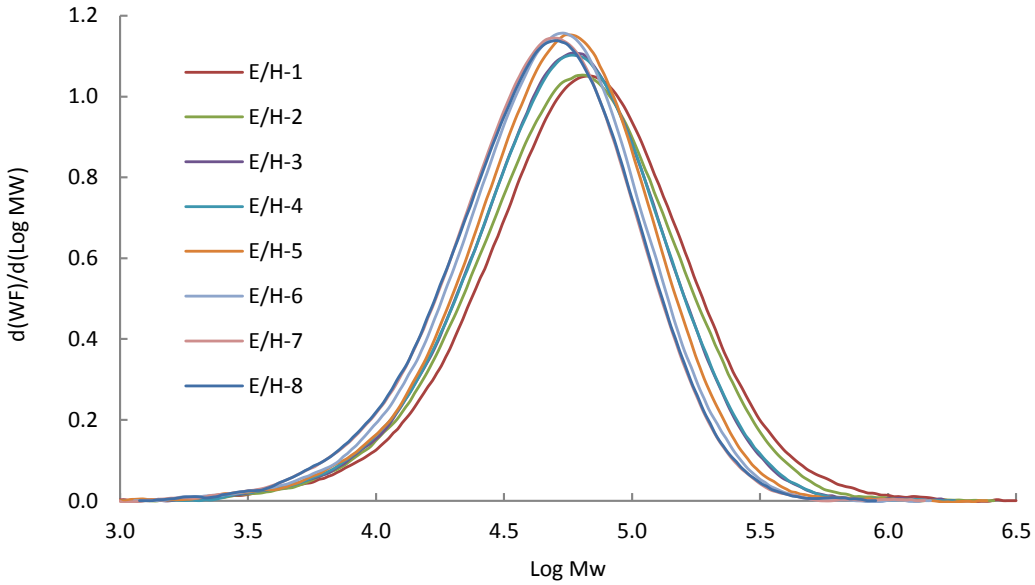

Figure 4-8. MWD of ethylene/1-hexene copolymer samples made with various comonomer contents.

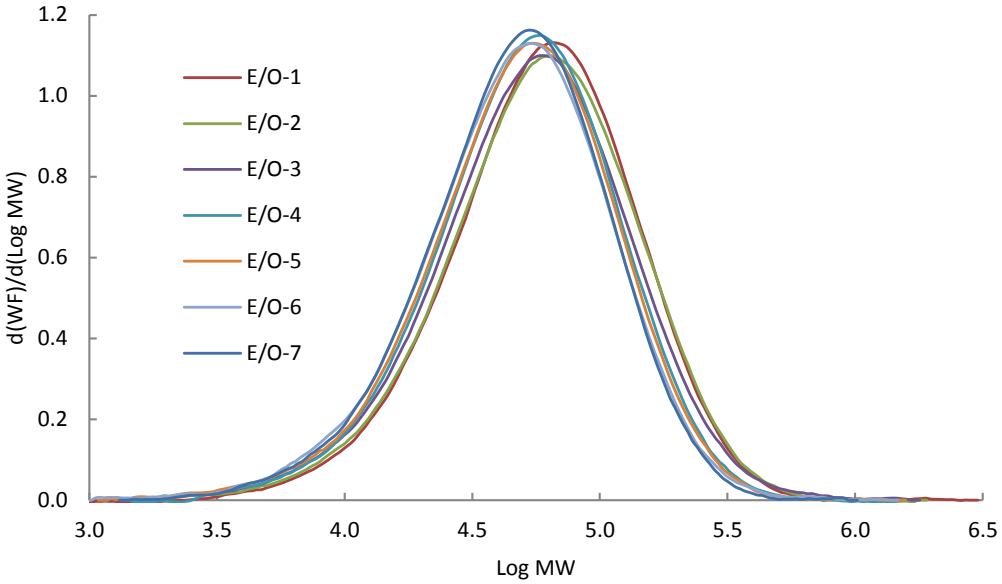

Figure 4-9. MWD of ethylene/1-octene copolymer samples made with various comonomer contents.

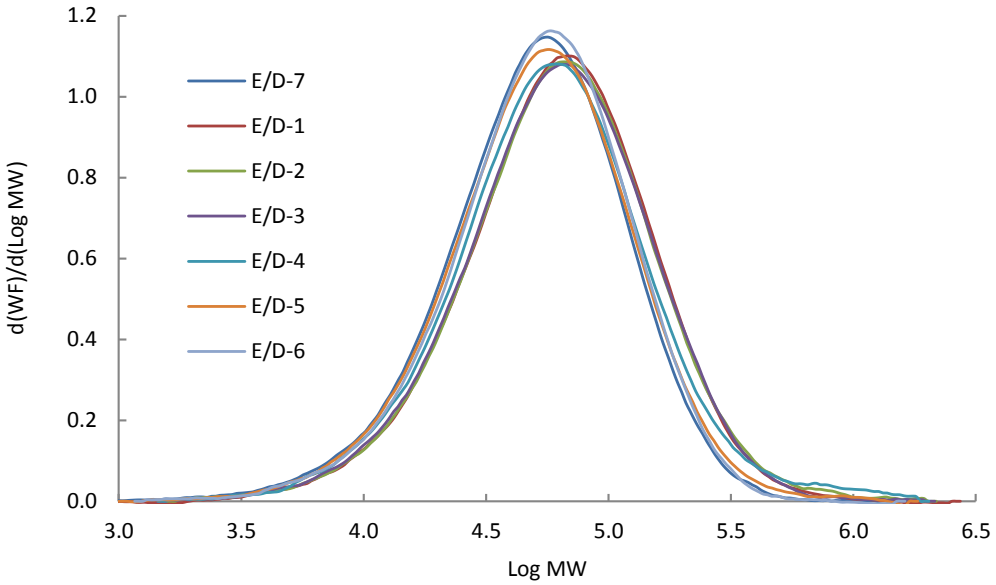

Figure 4-10. MWD of ethylene/1-dodecene copolymer samples made with various comonomer contents.

The comonomer mole fraction in the copolymer increases along with the comonomer concentration in the reactor as is shown in Figure 4-11, as expected. Furthermore, shorter comonomers such as 1-hexene are more easily incorporated than longer comonomers such as 1-dodecene, likely due to steric reasons, as also conveyed in Figure 4-11.

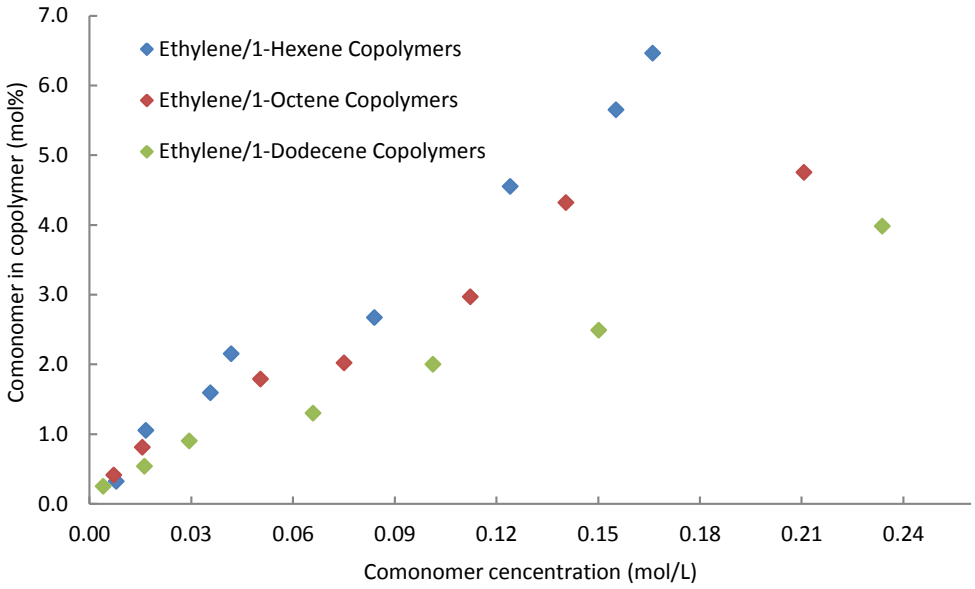

Figure 4-11. Relation between comonomer concentrations in copolymer and in the reactor.

The number average molecular weight (M_n) values displayed in Figure 4-12 and Figure 4-13 show that M_n decreases with increasing comonomer molar fraction in the copolymer and comonomer concentration in the reactor. Interestingly, Figure 4-12 shows that, despite comonomer type, copolymers with the same comonomer molar fraction have approximately the same M_n. On the other hand, Figure 4-13 shows that, at a given comonomer concentration in the reactor, M_n decreases more for shorter than for longer α-olefins, which are also more easily incorporated into the copolymer chains. Therefore, it seems that, at least for the catalyst used to make these copolymers, after an α-olefin molecule is incorporated into the polymer chain, the likelihood of chain transfer taking place is the same, regardless on the comonomer length.

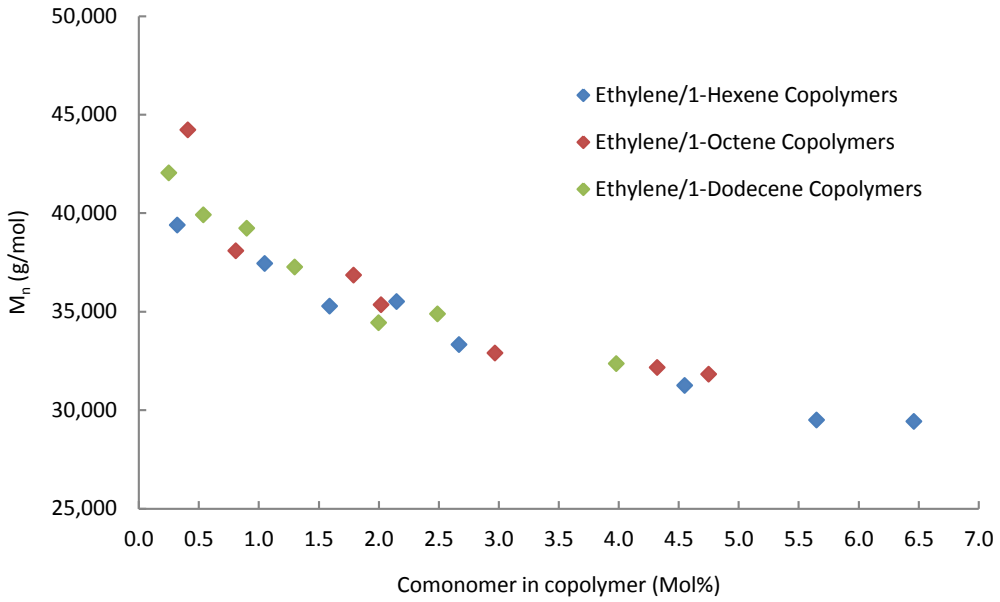

Figure 4-12. Effect of comonomer incorporation on the M_n of ethylene/α-olefin copolymers.

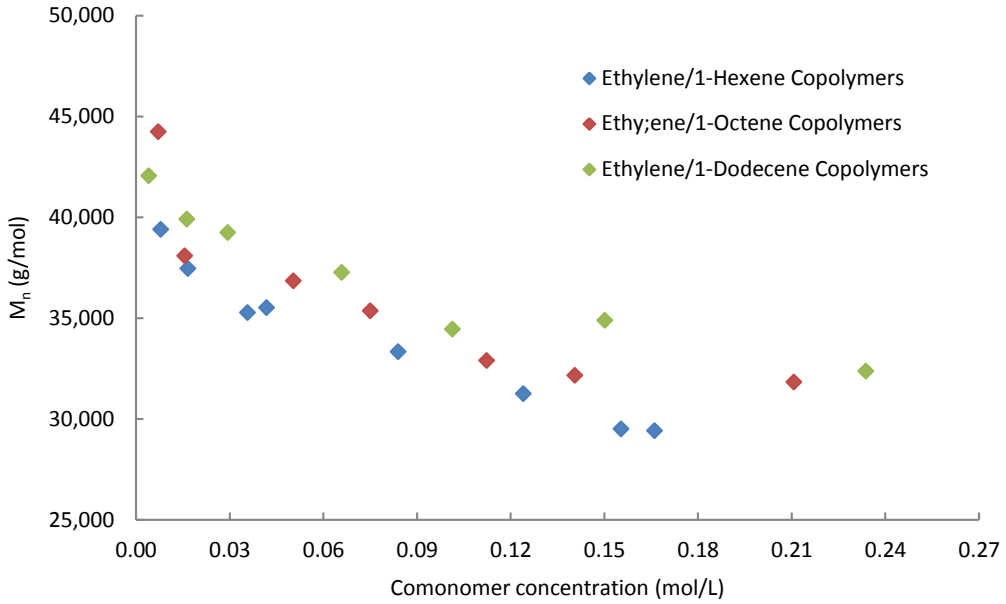

Figure 4-13. Effect of comonomer reactor concentration on the M_n of ethylene/ α-olefin copolymers.

4.2.5 Thermal Analysis

Ethylene/α-olefin copolymer samples were analyzed with DSC to determine the melting temperature and the degree of crystallinity as shown in Figure 4-14 for sample E/H-5. DSC results were already presented in Table 4-4, Table 4-5, and Table 4-6. Melting temperature and degree of crystallinity decrease steadily as SCB/1000 C increases in the copolymers, as indicated in Figure 4-15, Figure 4-16, and Figure 4-17. As expected, the melting temperature for ethylene/1-hexene copolymer is higher than ethylene/1-dodecene copolymer when they have the same comonomer mole fraction because copolymers having shorter chain branches are less effective in decreasing the copolymer melting point and co-crystallization is more likely to occur. Linear relationships are observed between the melting temperature and comonomer mole fraction, as depicted in Figure 4-15, Figure 4-16, and Figure 4-17.

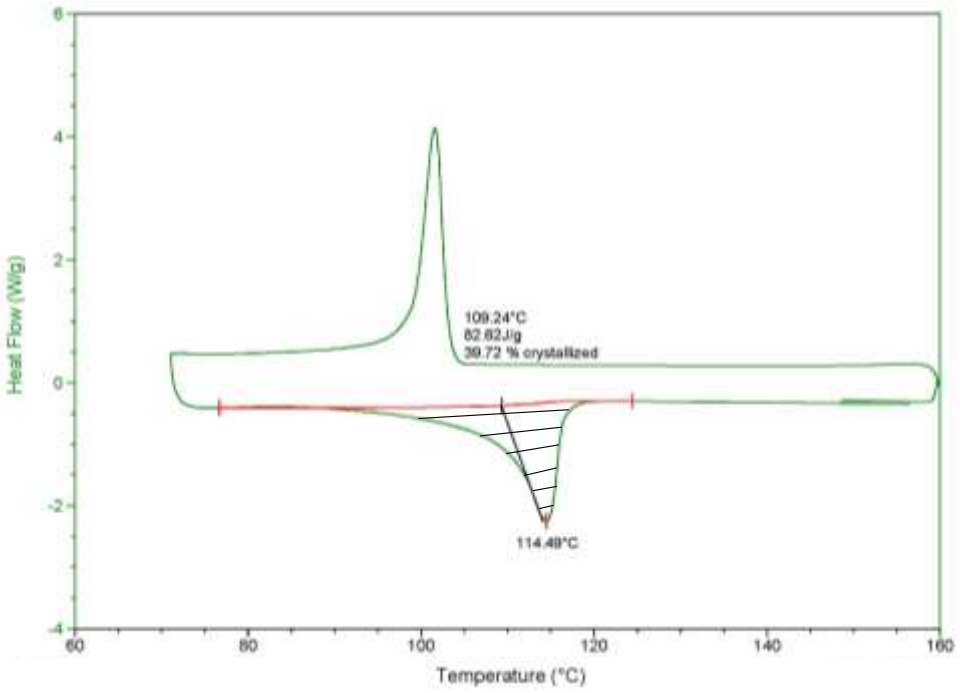

Figure 4-14. E/H-5 sample analyzed by DSC for determining the melting temperature and the degree of crystallinity.

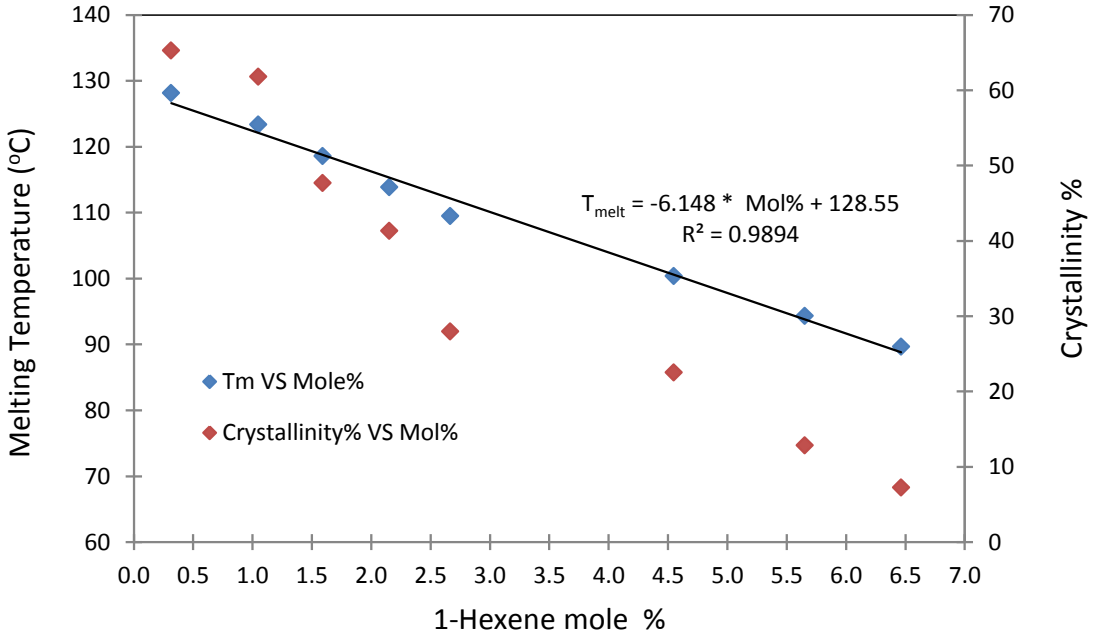

Figure 4-15. T_m and crystallinity % versus 1-Hexene mole %.

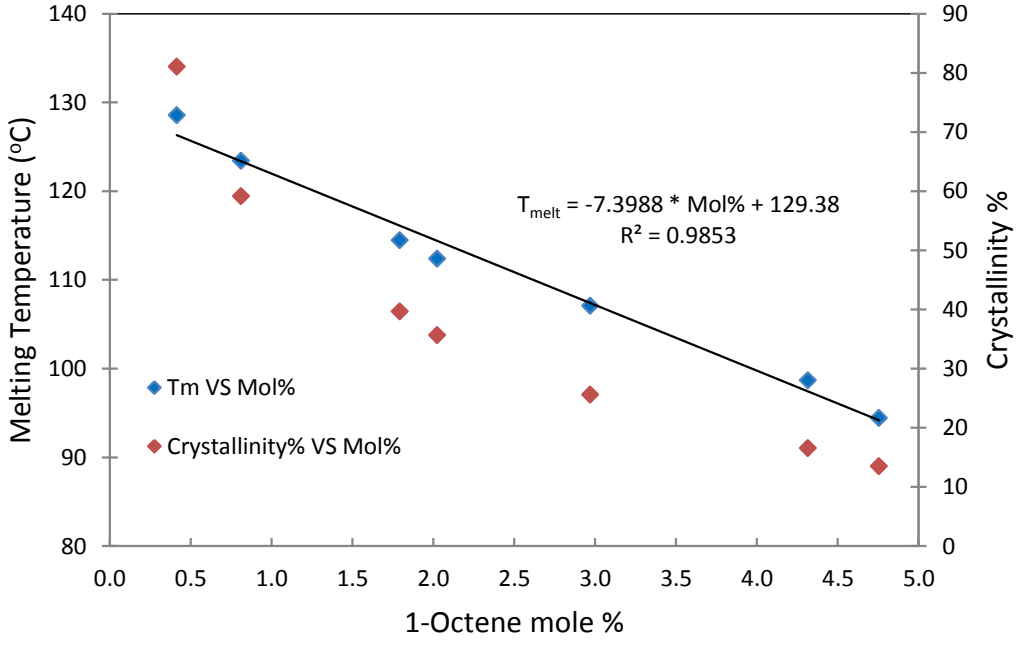

Figure 4-16. T_m and crystallinity % versus 1-Octene mole %.

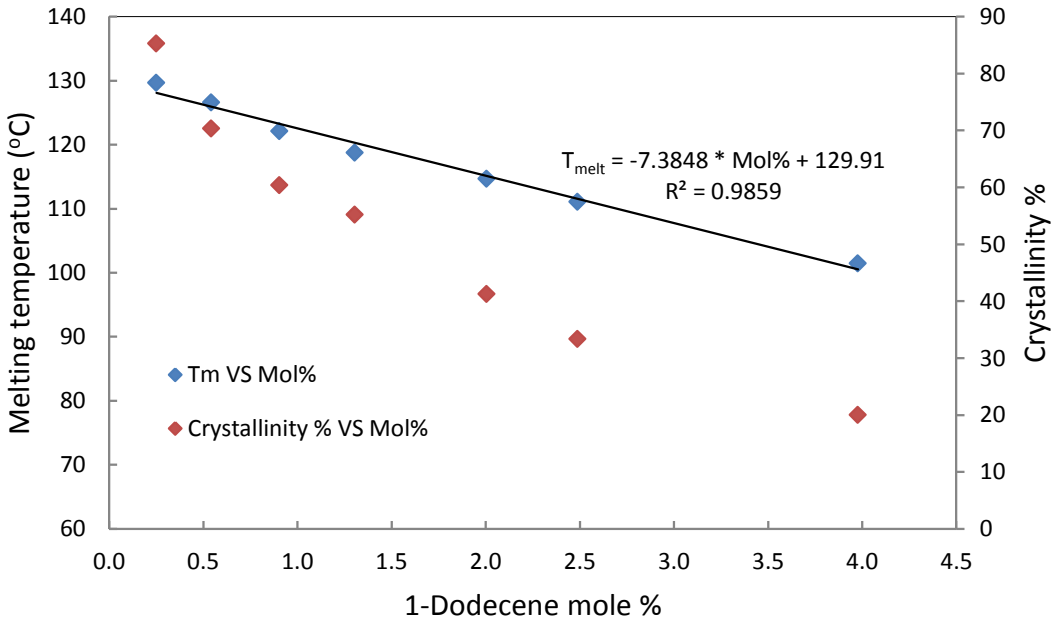

Figure 4-17. T_m and crystallinity % versus 1-Dodecene mole %

.

4.3 CEF Calibration Curve

Linear CEF calibration curves for ethylene/1-hexene, ethylene/1-octene and ethylene/1-dodecene copolymers are shown in Figure 4-18, Figure 4-19, and Figure 4-20, respectively, and shown below with their coefficients of correlation,

$$\textit{1-Hexene mole } \% = -0.1558 * T_{peak} + 15.302 \qquad (4.2)$$
$$R^2 = 0.9962$$

$$\textit{1-Octene mole } \% = -0.1346 * T_{peak} + 13.313 \qquad (4.3)$$
$$R^2 = 0.9957$$

$$\textit{1-Dodecene mole } \% = -0.1345 * T_{peak} + 13.291 \qquad (4.4)$$
$$R^2 = 0.9954$$

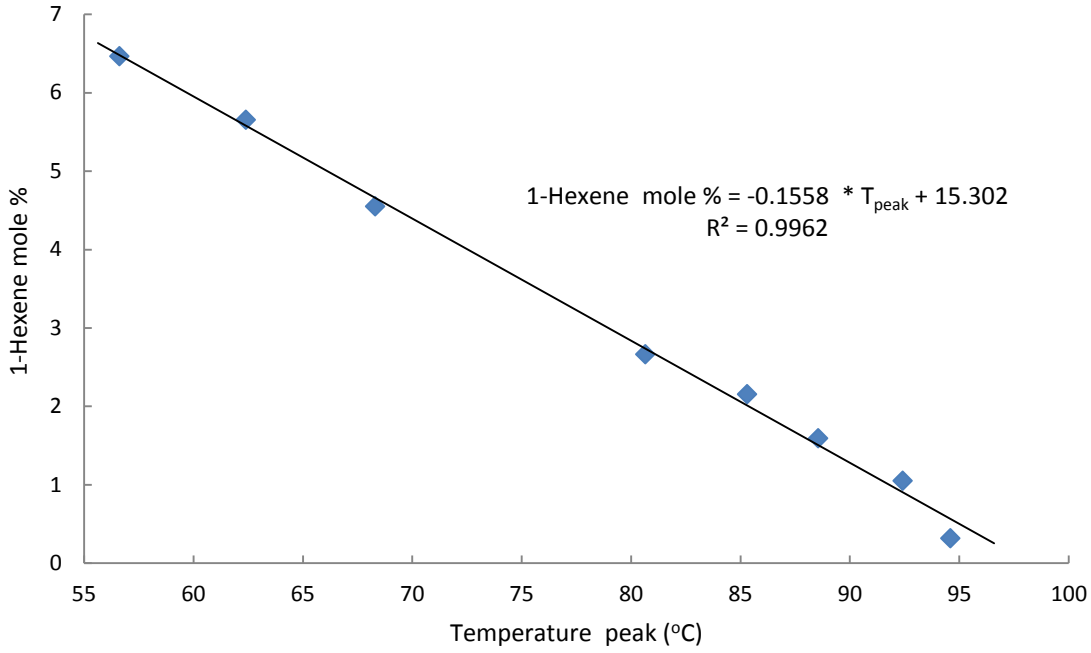

Figure 4-18. CEF calibration curve for ethylene/1-hexene copolymer.

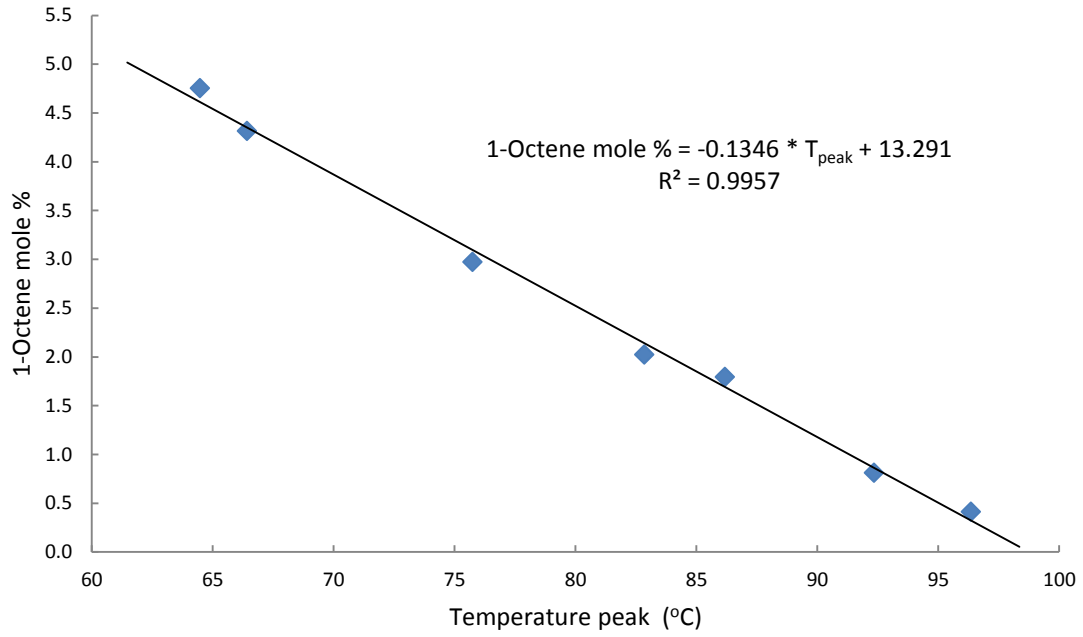

Figure 4-19. CEF calibration curve for ethylene/1-octene copolymer.

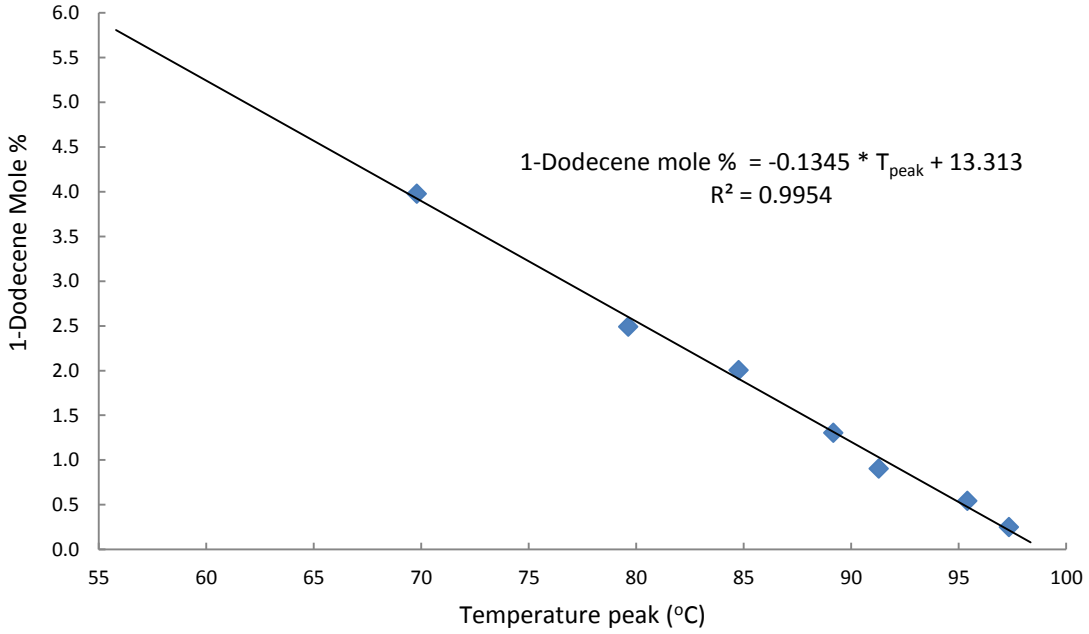

Figure 4-20. CEF calibration curve for ethylene/1-dodecene copolymer.

Figure 4-21 presents the calibration curves for all the copolymer samples used in this thesis. The curve slope for ethylene/1-hexene copolymers is higher those for ethylene/1-octene and ethylene/1-dodecene copolymers. This means that butyl branches are less effective in disrupting the crystallizability of the copolymer chains than hexyl or decyl branches, perhaps because butyl branches can be partially incorporated into the crystal lattice. On the other hand, the calibration curves for ethylene/1-octene and ethylene/1-dodecene copolymers are the same. implying that CEF elution temperature is independent of α-olefin length for α-olefin longer than 1-octene, at least up to the point where the SCB become large enough to start crystallizing themselves. Similar observations have been made for CRYSTAF and TREF.(Monrabal et al., 1999; Sarzotti et al., 2002; Anantawaraskul et al., 2005)

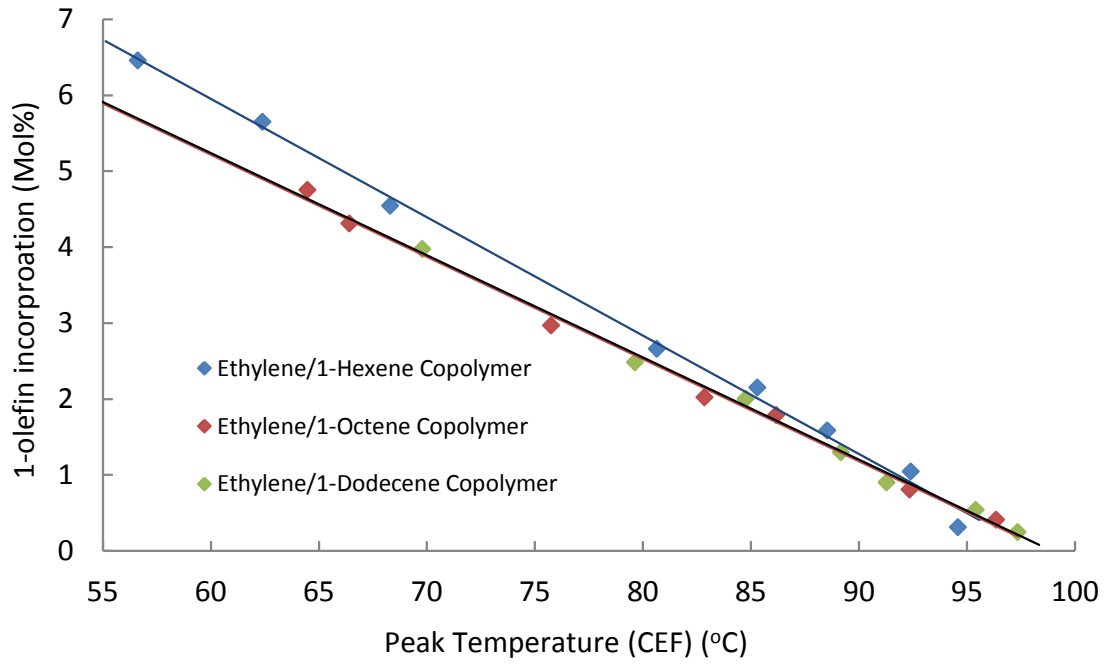

Figure 4-21. CEF calibration curve for ethylene/α-olefin copolymer.

Interestingly, the slopes of the calibration curve for CEF and DSC for all ethylene/α-olefin copolymer samples used in this thesis are about the same, producing the parallel lines presented in Figure 4-22, Figure 4-23, and Figure 4-24. The differences between the elution peak temperatures in CEF and the melting temperatures in DSC ($\Delta T = T_{DSC} - T_{CEF}$) have an average of 30.7 °C, as shown in Figure 4-25. Therefore, at least for these single-site resins, T_m measured by DSC can be used to estimate the peak elution temperature in CEF, and vice-versa.

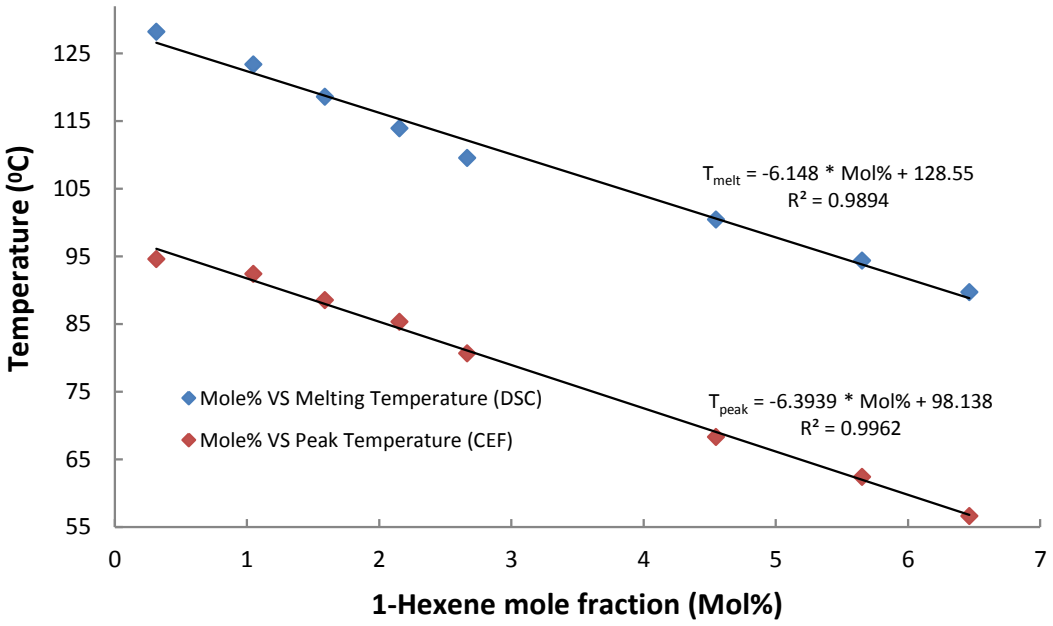

Figure 4-22. CEF and DSC calibration curves for ethylene/1-hexene copolymer.

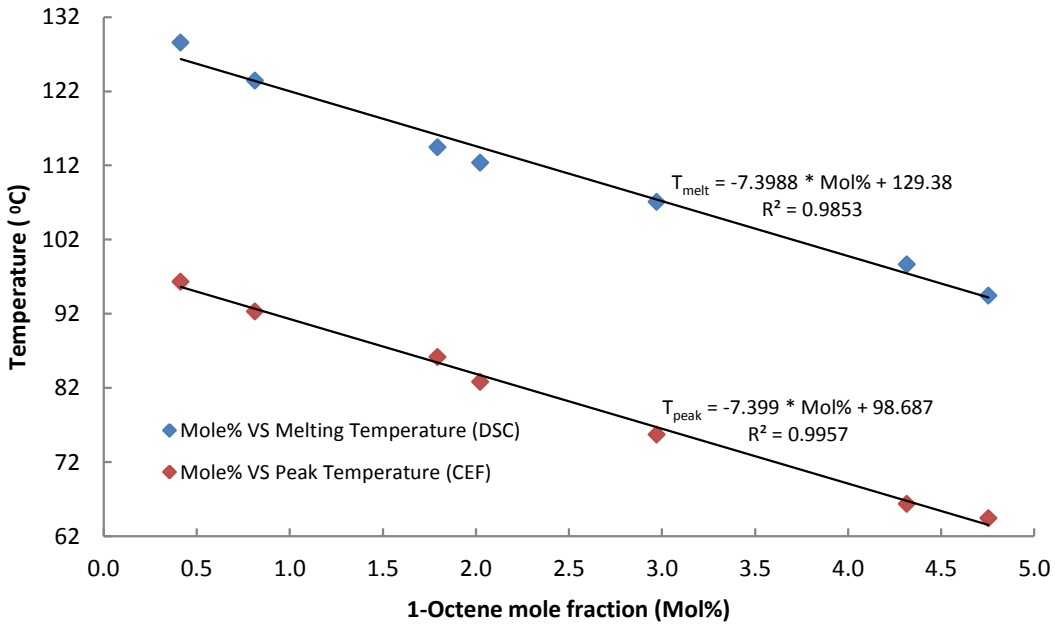

Figure 4-23. CEF and DSC calibration curves for ethylene/1-octene copolymer.

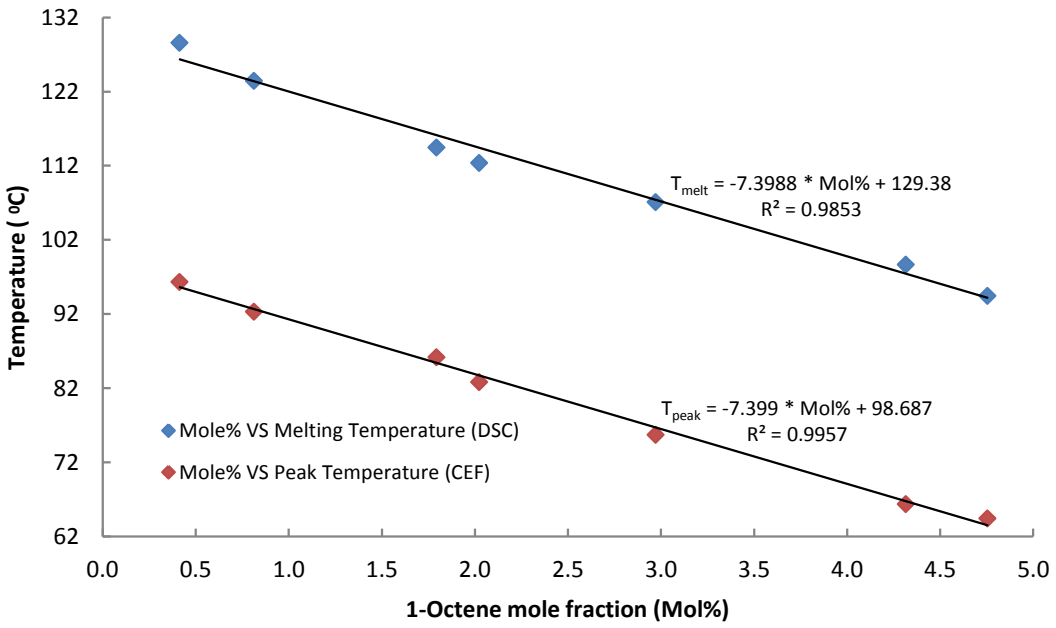

Figure 4-24. CEF and DSC calibration curves for ethylene/1-dodecene copolymer.

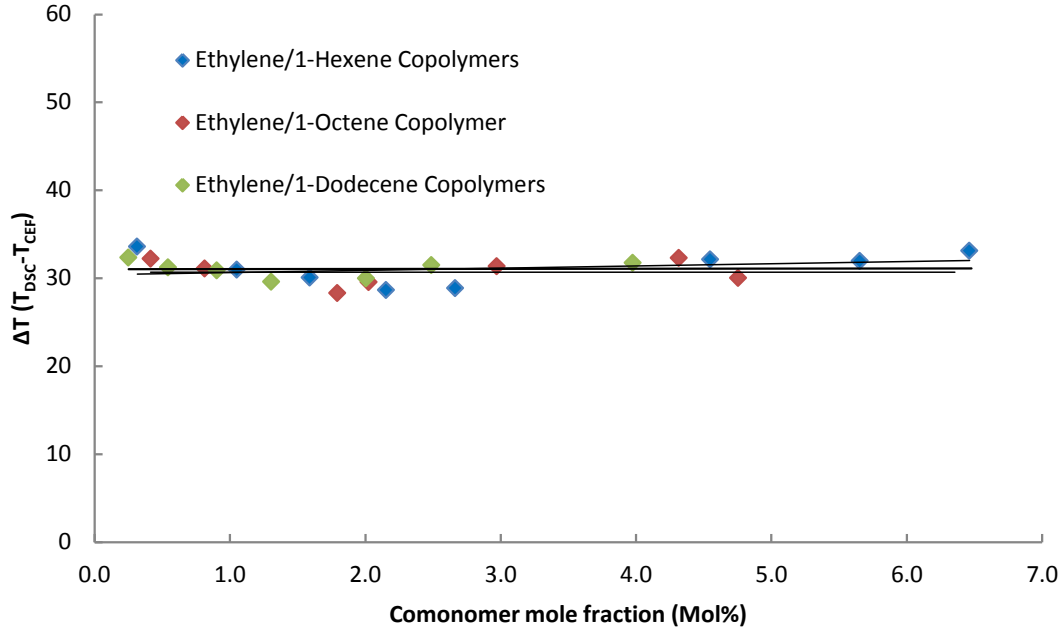

Figure 4-25. ΔT (T_{DSC}- T_{CEF}) for all copolymer samples.

Chapter 5- Conclusions and Recommendations

CEF is becoming the most important CCD characterization technique in polyolefin laboratories because it has shorter analysis times and higher resolution than TREF and CRYSTAF.

The method used to generate the calibration curves in this thesis required the CEF analysis of several narrow CCD samples, each with known comonomer contents synthesized with single site catalysts, covering a broad range of crystallization temperatures. It was found out that CEF calibration curves for ethylene/α-olefin copolymer are linear, similarly to TREF and CRYSTAF. Also similar to CRYSTAF and TREF, CEF elution peak temperatures become independent on comonomer type for α-olefins longer than 1-hexene.

These calibration curves can be useful for quantifying the CCD of unknown copolymers from their respective crystallizability distributions. Since these calibration curves are not universal, it is generally required that the unknown and standard polymers have the same comonomer type and follow similar copolymerization statistics. Since there are kinetic considerations involved in the crystallization process, the calibration curves can be used for identification of the unknown polymers' CCD, provided that these samples are collected at the same crystallization rate as the original standard samples (already known as analyzed by CEF). In addition, the calibration curves can be utilized for ethylene/α-olefin copolymers with up to 6.4 % of comonomer.

The melting temperature of ethylene/α-olefin copolymer is decreasing with increasing the comonomer content in polymer. More interestingly, CEF can be easily used to estimate the melting temperature for ethylene/α-olefin copolymer samples since the average differences between the crystallization peak temperature (T_{CEF}) analyzed by CEF and melting temperature (T_{DSC}) determined by DSC ($\Delta T = T_{DSC} - T_{CEF}$) is equal to 30.7 ^{o}C.

Some recommendations for future work are:

- Establishing calibration curves for ethylene/1-propylene copolymer (shortest SCB) and also for ethylene/1-eicosene copolymer to widen the range of SCB length.

- More interestingly, generating calibration curves for ethylene copolymerization with nonlinear branches is a challenging subject that can be considered by CEF technique.

- It is interesting to use other methods such as providing a group of preparative TREF fractions from broad-CCD Ziegler–Natta copolymers and comparing the results with the calibration curves that have been established in this thesis.

- Since the calibration curves of CEF depend on cooling rate, and crystallization and elution flow rates used to analyze the samples, it would be interesting to vary these rates to find out how they affect peak separation and calibration curves.

Appendix A

^{13}C NMR spectra of ethylene/α-olefin copolymer samples (E/H-1, E/H-5, E/H-6, and E/O-4) made with different comonomer fractions.

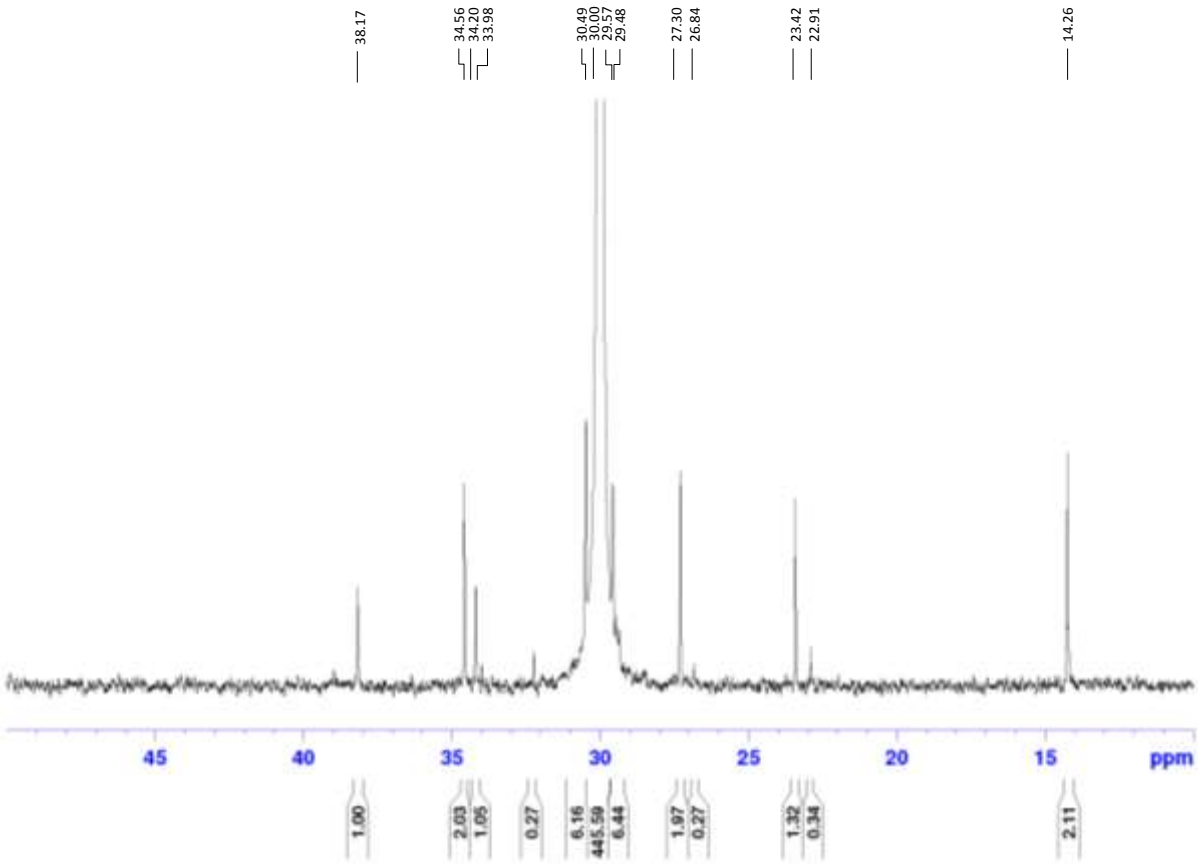

Figure 5-1. ^{13}C NMR spectra of ethylene/1-hexene copolymer, containing 0.32 % 1-hexene, E/H-1.

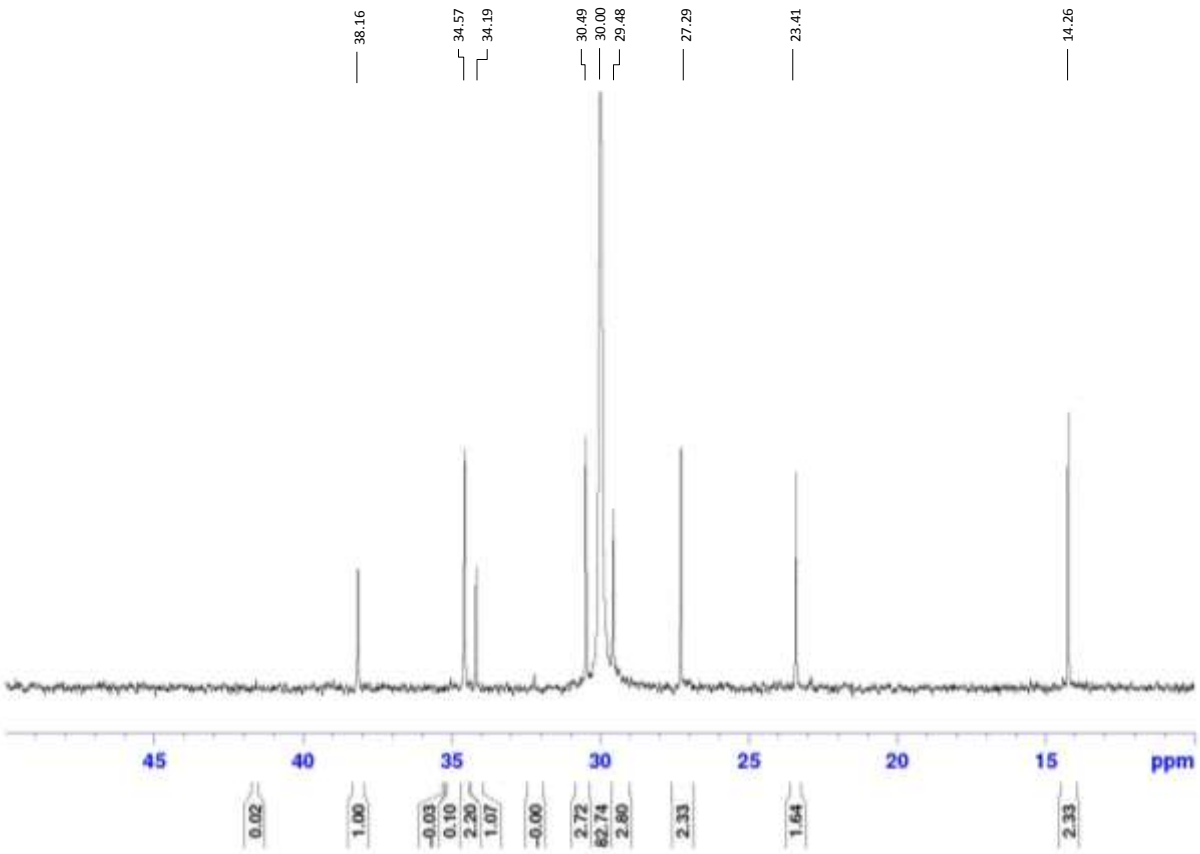

Figure 5-2. ^{13}C NMR spectra of ethylene/1-hexene copolymer, containing 2.67 % 1-hexene, E/H-5.

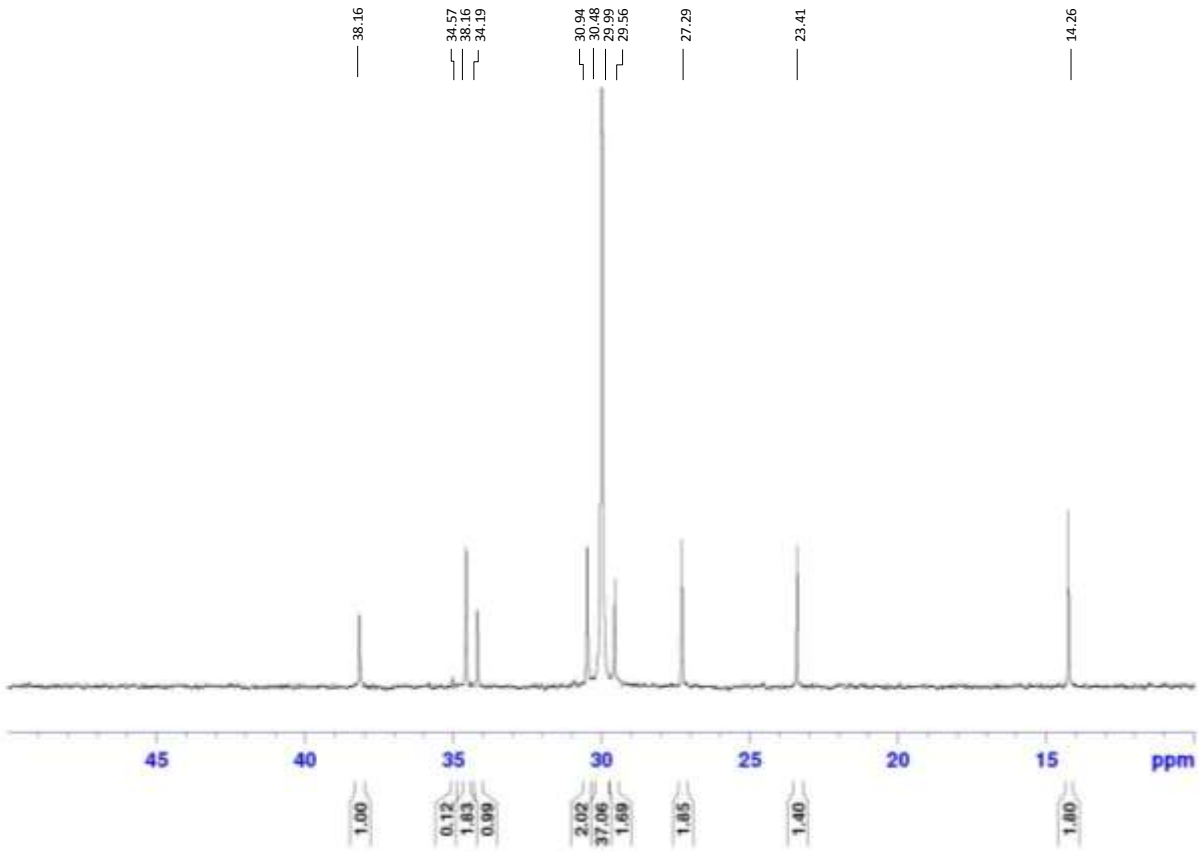

Figure 5-3. ^{13}C NMR spectra of ethylene/1-hexene copolymer, containing 4.55 % 1-hexene, E/H-6.

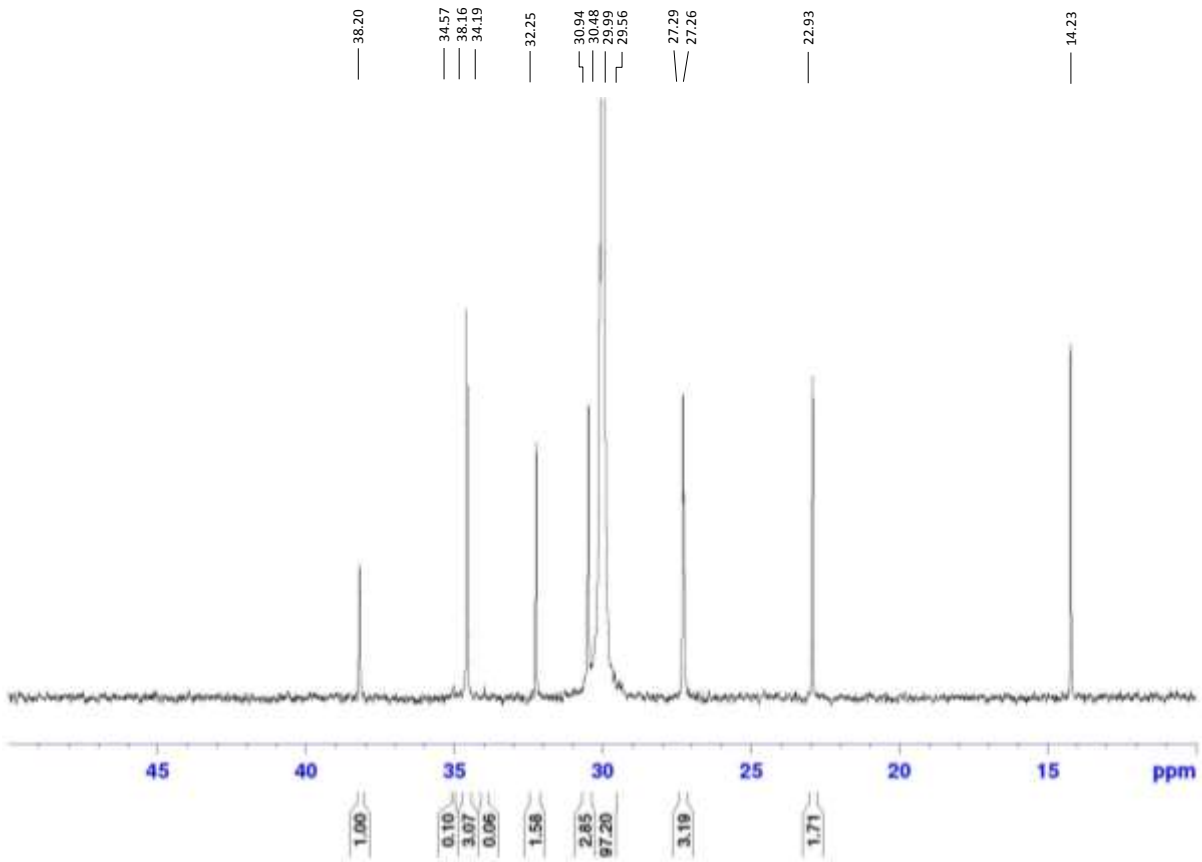

Figure A-4. ^{13}C NMR spectra of ethylene/1-octene copolymer, containing 2.02 % 1-octene, E/O-4.

Bibliography

Anantawaraskul, Siripon; Soares, João; Wood-Adams, Paula, 2005. Fractionation of Semicrystalline Polymers by Crystallization Analysis Fractionation and Temperature Rising Elution Fractionation. Polymer Analysis Polymer Theory, *Springer Berlin / Heidelberg*. **182:** 686-686.

Anantawaraskul, Siripon; Somnukguandee, Punnawit; Soares, João B. P.; Limtrakul, Jumras, 2009. Application of a crystallization kinetics model to simulate the effect of operation conditions on Crystaf profiles and calibration curves, *Journal of Polymer Science Part B: Polymer Physics*, **47**,(9): 866-876.

Arnal, M.; Balsamo, V.; Ronca, G.; Sánchez, A.; Müller, A.; Cañizales, E.; Urbina de Navarro, C., 2000. Applications of Successive Self-Nucleation and Annealing (SSA) to Polymer Characterization, *Journal of Thermal Analysis and Calorimetry*, **59**,(1): 451-470.

ASTM-D5017-96, American Society for Testing and Materials, 2009. Standard Test Method for Determination of Linear Low Dinsity Polyethylene (LLDPE) Composition by Carbon-13 Nuclear Magnetic Resonance. United States, American Society for Testing and Materials, *ASTM D5017-96*.

ASTM-D6645-1, American Society for Testing and Materials, 2010. Standard Test Method for Methyl (Comonomer) Content in Polyethylene by Infrared Spectrophotometry, *ASTM D6645-1*.

Barlow, A.; Wild, L.; Ranganath, R., 1977. Gel permeation chromatography of polyethylene. I. Calibration, *Journal of Applied Polymer Science*, **21**,(12): 3319-3329.

Blitz, Jonathan P.; McFaddin, Douglas C., 1994. The characterization of short chain branching in polyethylene using fourier transform infrared spectroscopy, *Journal of Applied Polymer Science*, **51**,(1): 13-20.

Bubeck, R. A., 2002. Structure-property relationships in metallocene polyethylenes, *Materials Science and Engineering: R: Reports*, **39**,(1): 1-28.

De Pooter, M.; Smith, P. B.; Dohrer, K. K.; Bennett, K. F.; Meadows, M. D.; Smith, C. G.; Schouwenaars, H. P.; Geerards, R. A., 1991. Determination of the composition of common linear low density polyethylene copolymers by 13C-NMR spectroscopy, *Journal of Applied Polymer Science*, **42**,(2): 399-408.

Epacher, Edina; Kröhnke, Christoph; Pukánszky, Béla, 2000. Effect of catalyst residues on the chain structure and properties of a Phillips type polyethylen, *Polymer Engineering & Science*, **40**,(6): 1458-1468.

Gulmine, J. V.; Janissek, P. R.; Heise, H. M.; Akcelrud, L., 2002. Polyethylene characterization by FTIR, *Polymer Testing*, **21**,(5): 557-563.

Kaminsky, W.; Laban, A., 2001. Metallocene catalysis, *Applied Catalysis A: General*, **222**,(1-2): 47-61.

Kaminsky, Walter, 1998. Highly active metallocene catalysts for olefin polymerization, *Journal of the Chemical Society, Dalton Transactions*,(9): 1413-1418.

Kaminsky, Walter; Hoff, Matthias; Derlin, Stefanie, 2007. Tailored Branched Polyolefins by Metallocene Catalysis, *Macromolecular Chemistry and Physics*, **208**,(13): 1341-1348.

Kaminsky, Walter; Piel, Christian; Scharlach, Katrin, 2005. Polymerization of Ethene and Longer Chained Olefins by Metallocene Catalysis, *Macromolecular Symposia*, **226**,(1): 25-34.

Krimm, S., 1978. Polymer sequence determination, carbon-13 NMR method, James C. Randall, Academic, New York, 1977, 155 pp, *Journal of Polymer Science: Polymer Letters Edition*, **16**,(9): 481-481.

Mara, J. J.; Menard, K. P., 1994. Characterization of linear low density polyethylene by temperature rising elution fractionation and by differential scanning calorimetry, *Acta Polymerica*, **45**,(5): 378-380.

Menczel, Joseph D.; Judovits, Lawrence; Prime, R. Bruce; Bair, Harvey E.; Reading, Mike; Swier, Steven, 2008. Differential Scanning Calorimetry (DSC). Thermal Analysis of Polymers, *John Wiley & Sons, Inc.***:** 7-239.

Monrabal, B.; Romero, L.; Mayo, N.; Sancho-Tello, J., 2009. Advances in Crystallization Elution Fractionation, *Macromolecular Symposia*, **282**,(1): 14-24.

Monrabal, B.; Sancho-Tello, J.; Mayo, N.; Romero, L., 2007. Crystallization Elution Fractionation. A New Separation Process for Polyolefin Resins, *Macromolecular Symposia*, **257**,(1): 71-79.

Monrabal, Benjamin, 1996. Crystaf: Crystallization analysis fractionation. A new approach to the composition analysis of semicrystalline polymers, *Macromolecular Symposia*, **110**,(1): 81-86.

Monrabal, Benjamín; Blanco, Javier; Nieto, Jesús; Soares, João B. P., 1999. Characterization of homogeneous ethylene/1-octene copolymers made with a single-site catalyst. CRYSTAF analysis and calibration, *Journal of Polymer Science Part A: Polymer Chemistry*, **37**,(1): 89-93.

Moore, J. C., 1964. Gel permeation chromatography. I. A new method for molecular weight distribution of high polymers, *Journal of Polymer Science Part A: General Papers*, **2**,(2): 835-843.

Mortazavi, S. Mohammad M.; Arabi, Hassan; Zohuri, Gholamhossein; Ahmadjo, Saeid; Nekoomanesh, Mehdi; Ahmadi, Mostafa, 2010. Copolymerization of ethylene/α-olefins using bis(2-phenylindenyl)zirconium dichloride metallocene catalyst: structural study of comonomer distribution, *Polymer International*, **59**,(9): 1258-1265.

Pasch, Harald, 2001. Recent developments in polyolefin characterization, *Macromolecular Symposia*, **165**,(1): 91-98.

Randall, James C., 1989. A Review of High Resolution Liquid Carbon-13 Nuclear Magnetic Resonance Characterization of Ethylene-Based Polymers, **29**,(2): 201 - 317.

Rudin, Alfred, 1999. Practical Aspects of Molecular Weight Measurements. Elements of Polymer Science and Engineering (Second Edition). San Diego, *Academic Press***:** 73-120.

Sarzotti, Deborah M.; Soares, João B. P.; Penlidis, Alexander, 2002. Ethylene/1-hexene copolymers synthesized with a single-site catalyst: Crystallization analysis fractionation, modeling, and reactivity ratio estimation, *Journal of Polymer Science Part B: Polymer Physics*, **40**,(23): 2595-2611.

Sarzotti, Deborah M.; Soares, João B. P.; Simon, Leonardo C.; Britto, Lucas J. D., 2004. Analysis of the chemical composition distribution of ethylene/[alpha]-olefin copolymers by solution differential scanning calorimetry: an alternative technique to Crystaf, *Polymer*, **45**,(14): 4787-4799.

Seger, Mark R.; Maciel, Gary E., 2004. Quantitative 13C NMR Analysis of Sequence Distributions in Poly(ethylene-*co*-1-hexene), *Analytical Chemistry*, **76**,(19): 5734-5747.

Shanks, R.; Amarasinghe, G., 2000. Comonomer Distribution in Polyethylenes Analysed by DSC After Thermal Fractionation, *Journal of Thermal Analysis and Calorimetry*, **59**,(1): 471-482.

Sinn, Hansjörg, 1995. Proposals for structure and effect of methylalumoxane based on mass balances and phase separation experiments, *Macromolecular Symposia*, **97**,(1): 27-52.

Soares, João B. P., 2001. Mathematical modelling of the microstructure of polyolefins made by coordination polymerization: a review, *Chemical Engineering Science*, **56**,(13): 4131-4153.

Soares, João B. P., 2004. Polyolefins with Long Chain Branches Made with Single-Site Coordination Catalysts: A Review of Mathematical Modeling Techniques for Polymer Microstructure, *Macromolecular Materials and Engineering*, **289**,(1): 70-87.

Soares, João B. P., 2007. An Overview of Important Microstructural Distributions for Polyolefin Analysis, *Macromolecular Symposia*, **257**,(1): 1-12.

Soares, João B. P.; Anantawaraskul, Siripon, 2005. Crystallization analysis fractionation, *Journal of Polymer Science Part B: Polymer Physics*, **43**,(13): 1557-1570.

Soares, João B. P.; McKenna, Timothy; Cheng, C. P., 2008. Coordination Polymerization. Polymer Reaction Engineering, *Blackwell Publishing Ltd***:** 29-117.

Soares, João B. P.; Simon, Leonardo C., 2008. Coordination Polymerization. Handbook of Polymer Reaction Engineering, *Wiley-VCH Verlag GmbH***:** 365-430.

Stadler, Florian J.; Takahashi, Tatsuhiro; Yonetake, Koichiro, 2011. Crystal structure of ethene-/[alpha]-olefin copolymers with various long comonomers (C_8-C_{26}), *European Polymer Journal*, **47**,(5): 1048-1053.

Starck, P.; Rajanen, K.; Löfgren, B., 2002. Comparative studies of ethylene-[alpha]-olefin copolymers by thermal fractionations and temperature-dependent crystallinity measurements, *Thermochimica Acta*, **395**,(1-2): 169-181.

Williams, T.; Ward, I. M., 1968. The construction of a polyethylene calibration curve for gel permeation chromatography using polystyrene fractions, *Journal of Polymer Science Part B: Polymer Letters*, **6**,(9): 621-624.

Wunderlich, Bernhard, 2005. Differential Scanning Calorimetry Thermal Analysis of Polymeric Materials, *Springer***:** 329-448.

Yoon, J. S.; Lee, D. H.; Park, E. S.; Lee, I. M.; Park, D. K.; Jung, S. O., 2000. Thermal and mechanical properties of ethylene/[alpha]-olefin copolymers produced over (2-MeInd)$_2$ZrCl$_2$/MAO system, *Polymer*, **41**,(12): 4523-4530.

Zhang, Qing; Chen, Ping; Xie, Xiaoli; Cao, Xianwu, 2009. An effective method to identify the type and content of α-olefin in polyolefine copolymer by Fourier Transform Infrared–Differential Scanning Calorimetry, *Journal of Applied Polymer Science*, **113**,(5): 3027-3032.